Supporting Information

Single cobalt atom catalysis for the construction of quinazolines and quinazolinones *via* the aerobic dehydrocyclization of ethanol

Xueping Zhang,[a] Kai Xu,[a] Yi Zhuang,[a] Shihao Yuan,[a] Yamei Lin,[b,c] Guo-Ping Lu[a*]

[a] School of Chemistry and Chemical Engineering, Nanjing University of Science and Technology, Nanjing 210094, China

[b] International Innovation Center for Forest Chemicals and Materials, Nanjing Forestry University, Nanjing 210037, China

[c] Nanjing Normal University, School of Food Science and Pharmaceutical Engineering, Nanjing, 210032, China

Table of Contents

1. General information

All chemical reagents were purchased from commercial suppliers and used directly without further purification. GC analyses were performed on an Agilent 7890A instrument (Column: Agilent 19091J-413: 30 m × 320 μm × 0.25 μm, carrier gas: H_2, FID detection. GC-MS was performed on an ISQ Trace 1300 in the electron ionization (EI) mode.

XRD analysis was performed on Shimadzu X-ray diffractometer (XRD-6000) with Cu Kα irradiation. Transmission electron microscopy (TEM) images were taken using a PHILIPS Tecnai 12 microscope operating at 120 kv. Scanning electron microscopy (SEM) images were performed using a Hitachi S-4800 apparatus on a sample powder previously dried and sputter-coated with a thin layer of gold. Atomic-resolution HAADF-STEM images were taken using a FEI Titan Cubed Themis G2 300 S/TEM with a probe corrector and a monochromator at 200 kV. X-ray photoelectron spectroscopy (XPS) was performed on an ESCALAB 250Xi spectrometer, using an Al Kα X-ray source (1350 eV of photons) and calibrated by setting the C 1s peak to 284.80 eV. Inductively coupled plasma mass spectrometry (ICP-MS) was analyzed on Optima 7300 DV. The electron paramagnetic resonance (EPR) signal of free radical spin was measured by Bruker EMXnano spectrometer. The photoluminescence spectra (PL) were analyzed on a HORIBA Scientific HR Evolution spectrophotometer with an excitation wavelength of 325 nm. BET surface area and pore size measurements were performed with N_2 adsorption/desorption isotherms at 77 K on a Micromeritics ASAP 2020 instrument. Before measurements, the samples were degassed at 150 °C for 12 h.

The X-ray absorption fine structure spectra (Zn K-edge) were collected at BL14W beamline in Shanghai Synchrotron Radiation Facility (SSRF). The storage rings of SSRF were operated at 3.5 GeV with a stable current of 200 mA. Using Si (111) double-crystal monochromator, the data collection was carried out in fluorescence mode using Lytle detector. All spectra were collected in ambient conditions. The Zn

K-edge XANES date were recorded in a transmission mode. Zn foil and ZnO were used as references. The acquired EXAFS date was extracted and processed according to the standard procedures using the ATHENA module implemented in the IFEFFIT software packages.

2. Recyclability test

In a typical recycling process, the recyclability of Co_1@NC-50 catalyst was investigated under the standard reaction conditions with a decreased reaction time of 2 h. The catalyst was collected by centrifugation after the reaction, washed by ethanol and dried under vacuum, and then reused in the next reaction cycle.

3. Calculation of k_H/k_D

The reaction orders were measured at 100 °C, and the reaction rate is assumed to follow the equation: [S1]

$$r = k \times [2-\text{aminobenzyl alcohol}]^{\alpha} \times [\text{ethanol}]^{\beta} \times [NH_3 \cdot H_2O]^{\gamma}$$

The the H/D kinetic isotope effect (KIE) experiment of the reactions was studied. Assuming that alkylation of acetophenone and benzyl alcohol follows the first reaction kinetics law, that is $\ln\left[\frac{1}{1-C}\right] = k(t-t_0)$, where C is approximately replaced by the conversion of acetophenone (mol %), k is the rate constant (min^{-1}), and t stands for reaction time (min), the a linear relationship between $-ln(1-C)$ and reaction time (min) was obtained, indicating that the reaction is first order with respect to benzyl alcohol [S1-S4]. The rate constants k of CH_3CH_2OH and CD_3CD_2OD at 100 °C were obtained, respectively, and the values of k_H/k_D were obtained by calculation

4. Calculation of TOF

TOF was calculated from the reaction rate derived by the number of Zn atoms exposed to the catalyst surface (eqs. 1 and 2): [S5]

$$TOF = n_0/tn_{cat} \qquad (1)$$

$$n_{cat} = m_{cat}\omega/M_{Co} \qquad (2)$$

where n_0 is the initial molar of substrate, c is the conversion of substrates at the reaction of t, n_{cat} is the molar of exposed Co atom, ω is the mass fraction of Co in

catalysts, M_{Co} is molar mass of Co.

5. XAFS data processing

The XAFS data were processed according to the standard procedures using the Athena module implemented in the IFEFFIT software packages. The EXAFS spectra were obtained by subtracting the post-edge background from the overall absorption and then normalizing with respect to the edge-jump step. Subsequently, the χ(k) data of were Fourier transformed to real (R) space using a hanging window (dk = 1.0 Å−1) to separate the EXAFS contributions from different coordination shells. To obtain the quantitative structural parameters around central atoms, least-squares curve parameter fitting was performed using the ARTEMIS module of IFEFFIT software packages [S6,S7].

6. Computational details

Density functional theory (DFT) calculations were conducted using the Vienna *ab initio* simulation package (VASP) [S8,S9] with projector-augmented wave (PAW) method [S10]. The exchange-correlation effect was treated by the generalized gradient approximation (GGA) with the Perdew-Burke-Ernzerh (PBE) formalism [S11]. The energy cutoff for the plane-wave basis was set to 500 eV. A graphene p(4 × 4) supercell was employed with a lattice constant of 9.73 Å, and all surface slabs were modeled with a 20 Å vacuum layer. The Brillouin zone was sampled using 3 × 3 × 1 *k*-point grid for geometry relaxation. Conjugate gradient algorithms were utilized to optimize the position of all atoms and the lattice vectors, with convergence threshold was set to 10^{-6} eV and 0.02 eV/Å for energy and force, respectively.

The Gibbs free energy for was defined as:

$$G = E_{\mathrm{DFT}} + E_{\mathrm{ZPE}} - TS$$

where E_{DFT} is the DFT electronic energy, E_{ZPE} and S are the zero-point energy and the entropy at $T = 373.15$ K, which were obtained from the vibrational frequencies. During these frequency computations, all atoms of substrate were constrained.

To elucidate the hydrogen dissociation process, the transition states were identified

using the Climbing Nudged Elastic Band (CINEB) method implemented in the VASP-VTST code [S12]. Following the CINEB calculations, frequency analyses were conducted using a numerical algorithm with an atomic displacement of 0.015 Å. The presence of a single negative frequency confirmed the true transition state from the CINEB calculations.

7. Experimental procedure for the synthesis 6g

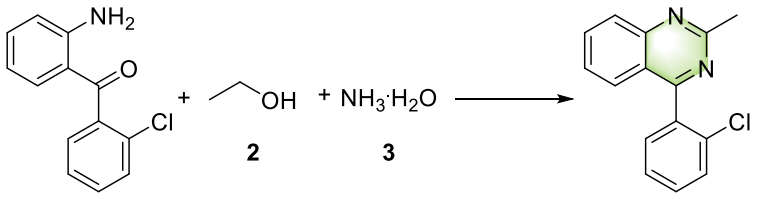

5g **2** **3** **6g**

5g (0.2 mmol), **2** (2 mL), **3** (1 mL) and Co_1@NC-50 (20 mg) were placed in a 25 mL sealed tube. Place the sealed tube in an oil bath preheated to 100 °C and the reaction was stirred for 6 h. After the reaction was completed, the sealed tube was cooled to room temperature, ethyl acetate was added to dilute the reaction mixture, and filtered through a bed of silica gel layered over Celite to obtain a reaction mixture liquid, which was concentrated under reduced pressure to obtain a crude product. Further purification through silica gel column chromatography using ethyl acetate/petroleum ether as eluant with gradually polarity increasing from 20% (ethyl acetate/petroleum ether, v/v = 2:8) to 70% (ethyl acetate/petroleum ether, v/v = 7:3). The yield of the pure product **6g** was 84% (42 mg).

8. Experimental procedure for the synthesis 8aa

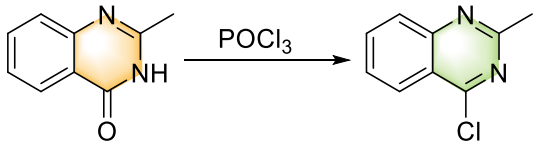

8a **8aa**

8a (0.5 mmol), N,N-diisopropylethylamine (1.5 eq.) and toluene (2 mL) were placed in a round bottom flask and refluxed for 1 h and then decreased to room temperature. Then put triphenylphosphine oxide (1.5 eq.) into the reaction solution, reacted at 80 °C for 2 h, diluted it with ethyl acetate after cooling, washed it with ice water, saturated $NaHCO_3$,

citric acid and saturated NaCl, and collected the organic layer. Furthermore, the organic layer was dried with anhydrous sodium sulfate, and the organic phase was concentrated under reduced pressure to obtain a crude product. Further purification through silica gel column chromatography using ethyl acetate/petroleum ether as eluant with gradually polarity increasing from 20% (ethyl acetate/petroleum ether, v/v = 2:8) to 70% (ethyl acetate/petroleum ether, v/v = 7:3). The yield of the pure product **8aa** was 61% (54 mg).

9. Experimental procedure for the synthesis 8ab

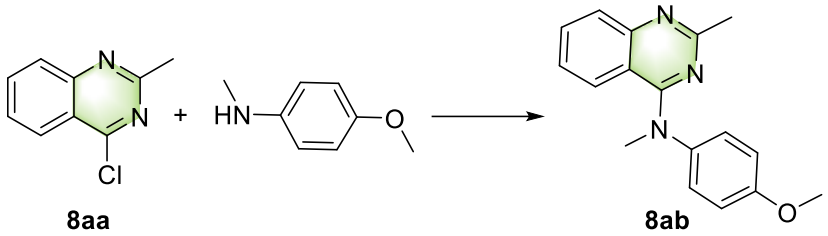

8aa **8ab**

8aa (0.5 mmol), 4-methoxy-N-methylaniline (1.1 eq.), hydrochloric acid (0.1 eq.) and anhydrous isopropanol (2 mL) were placed in the reactor and stirred 12 h at room temperature. After the reaction was completed, the solution was diluted with ethyl acetate, and filtered through a bed of silica gel layered over Celite to obtain a reaction mixture liquid, which was concentrated under reduced pressure to obtain a crude product. Further purification through silica gel column chromatography using ethyl acetate/petroleum ether as eluant with gradually polarity increasing from 20% (ethyl acetate/petroleum ether, v/v = 2:8) to 70% (ethyl acetate/petroleum ether, v/v = 7:3). The yield of the pure product 8ab was 63% (88 mg).

References

[S1] H. Wang, D. Y. Xu, E. Guan, L. Wang, J. Zhang, C. T. Wang, S. Wang, H. Xu, X. J. Meng, B. Yang, B. C. Gates, F. S. Xiao, Atomically dispersed Ru on manganese oxide catalyst boosts oxidative cyanation. *ACS Catal.* **2020**, *10*, 6299-6308.

[S2] W. P. Deng, Y. Z. Wang, S. Zhang, K. M. Gupta, M. J. Hülsey, H. Asakura, L. M. Liu, Y. Han, E. M. Karp, G. T. Beckham, P. J. Dyson, J. W. Jiang, T. Tanaka, Y. Wang, N. Yan, Catalytic amino acid production from biomass-derived intermediates. *PNAS* **2018**, *115*, 5093-5098.

[S3] F. Wang, W. Ueda, J. Xu, Detection and measurement of surface electron transfer on reduced molybdenum oxides (MoO_x) and catalytic activities of Au/MoO_x. *Angew. Chem. Int. Ed.* **2012**, *51*, 3883-3887.

[S4] J. L. Long, X. Q. Xie, J. Xu, Q. Gu, L. M. Chen, X. X. Wang, Nitrogen-doped graphene nanosheets as metal-free catalysts for aerobic selective oxidation of benzylic alcohols. *ACS Catal.* **2012**, *2*, 622-631.

[S5] R. J. Gao, L. Pan, H. W. Wang, X. W. Zhang, L. Wang, J. J. Zou, Ultradispersed nickel phosphide on phosphorus-doped carbon with tailored d-band center for efficient and chemoselective hydrogenation of nitroarenes. *ACS Catal.* **2018**, *8*, 8420-8429.

[S6] R. M. Newville, ATHENA, ARTEMIS, HEPHAESTUS: data analysis for X-ray absorption spectroscopy using IFEFFIT. *J Synchrotron. Radiat.* **2005**, *12*, 537-541.

[S7] S. I. Zabinsky, J. J. Rehr, A. Ankudinov, R. C. Albers, M. J. Eller, Multiple-scattering calculations of X-ray-absorption spectra. *Phys. Rev. B* **1995**, *52*, 2995-3009.

[S8] G. Kresse, J. Furthmüller, Efficient Iterative Schemes for ab initio Total-energy calculations using a plane-wave basis set. *Phys. Rev. B* **1996**, *54*, 11169-11186.

[S9] G. Kresse, J. Hafner, Ab initio molecular dynamics for liquid metals. *Phys. Rev. B Condens. Matter.* **1993**, *47*, 558-561.

[S10] P. E. Blöchl, Projector augmented-wave method. *Phys. Rev. B* **1994**, *50*, 17953-17979.

[S11] S. Grimme, S. Ehrlich, L. Goerigk, Effect of the damping function in dispersion corrected density functional theory. *J. Comput. Chem.* **2011**, *32*, 1456-1465.

[S12] G. Henkelman, B. P. Uberuaga, H. Jónsson, A climbing image nudged elastic band method for finding saddle points and minimum energy paths. *J. Chem. Phys.* **2000**, *113*, 9901-9904.

10. Results and discussion

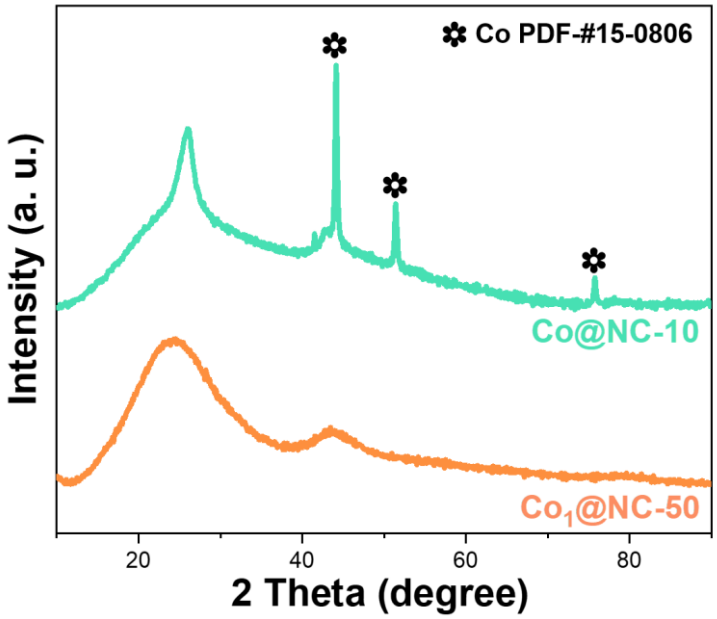

Figure S1 XRD pattern of Co@NC-10 and Co_1@NC-50.

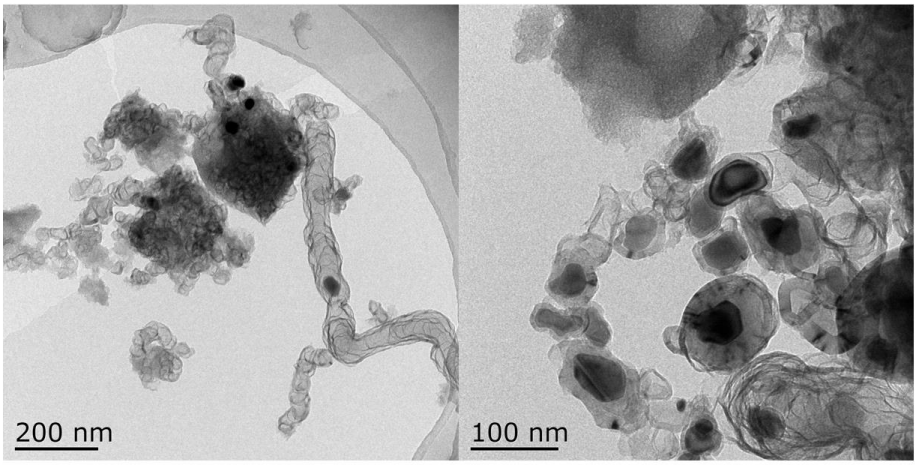

Figure S2 TEM of Co@NC-10.

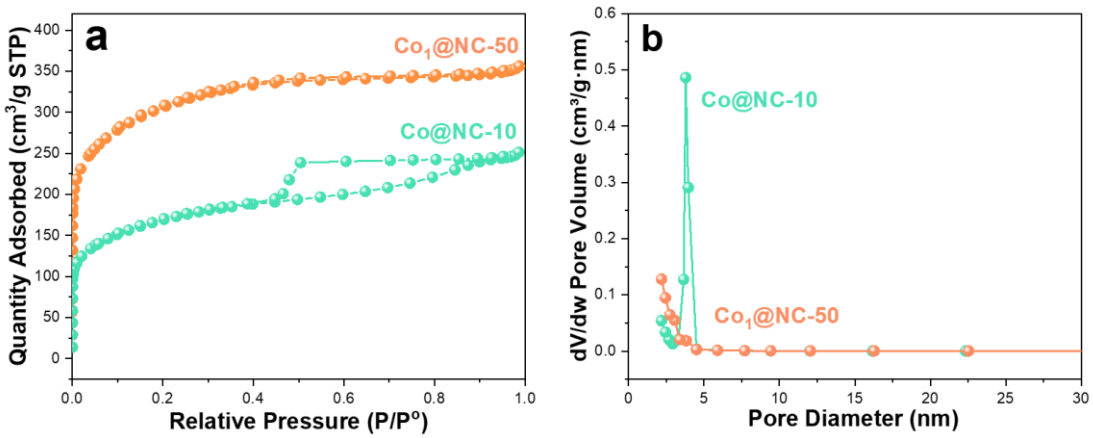

Figure S3 Adsorption isotherms of N_2 at 77 K with Co@NC-10 and Co_1@NC-50.

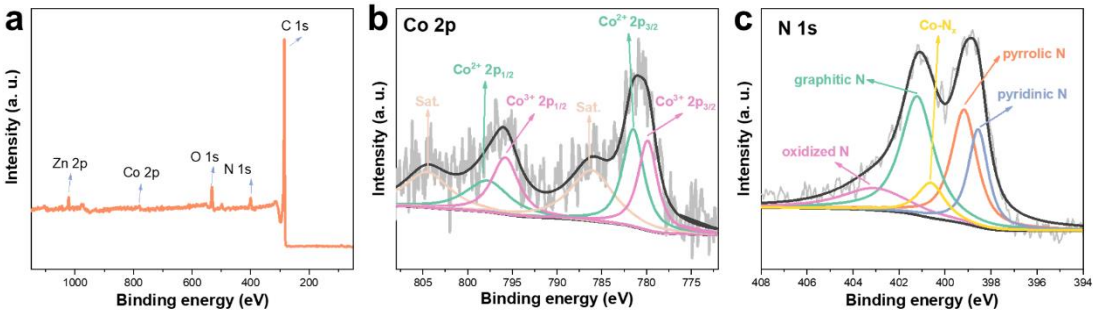

Figure S4 XPS spectra of Co_1@NC-50. (a) Survey spectrum, (b) Co 2p region (c) N 1s region and.

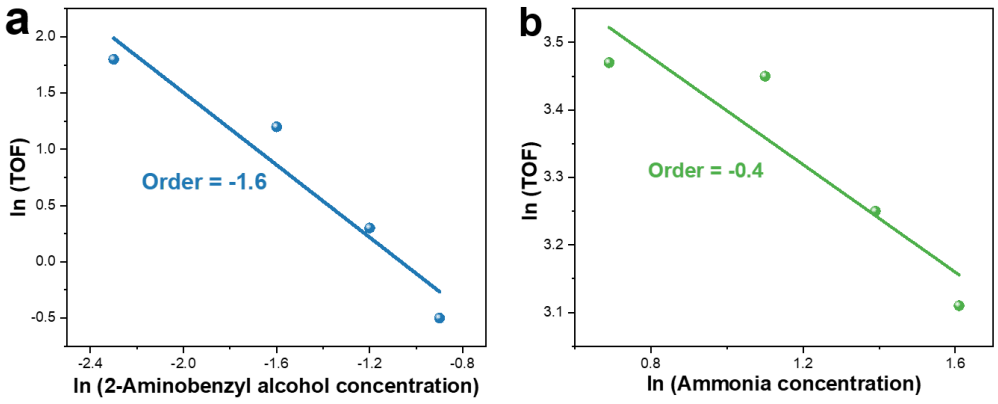

Figure S5 Plots determining reaction orders for the aerobic dehydrogenation cyclization of (a) 2-aminobenzyl alcohol and (b) ammonia. Reaction conditions: 0.1-0.4 mmol of 2-aminobenzyl alcohol, 2-5 mmol of ammonia, Co_1@NC-50 (2.5 mol%

Co), H_2O (1 mL), 100 °C, 0.5 h, air.

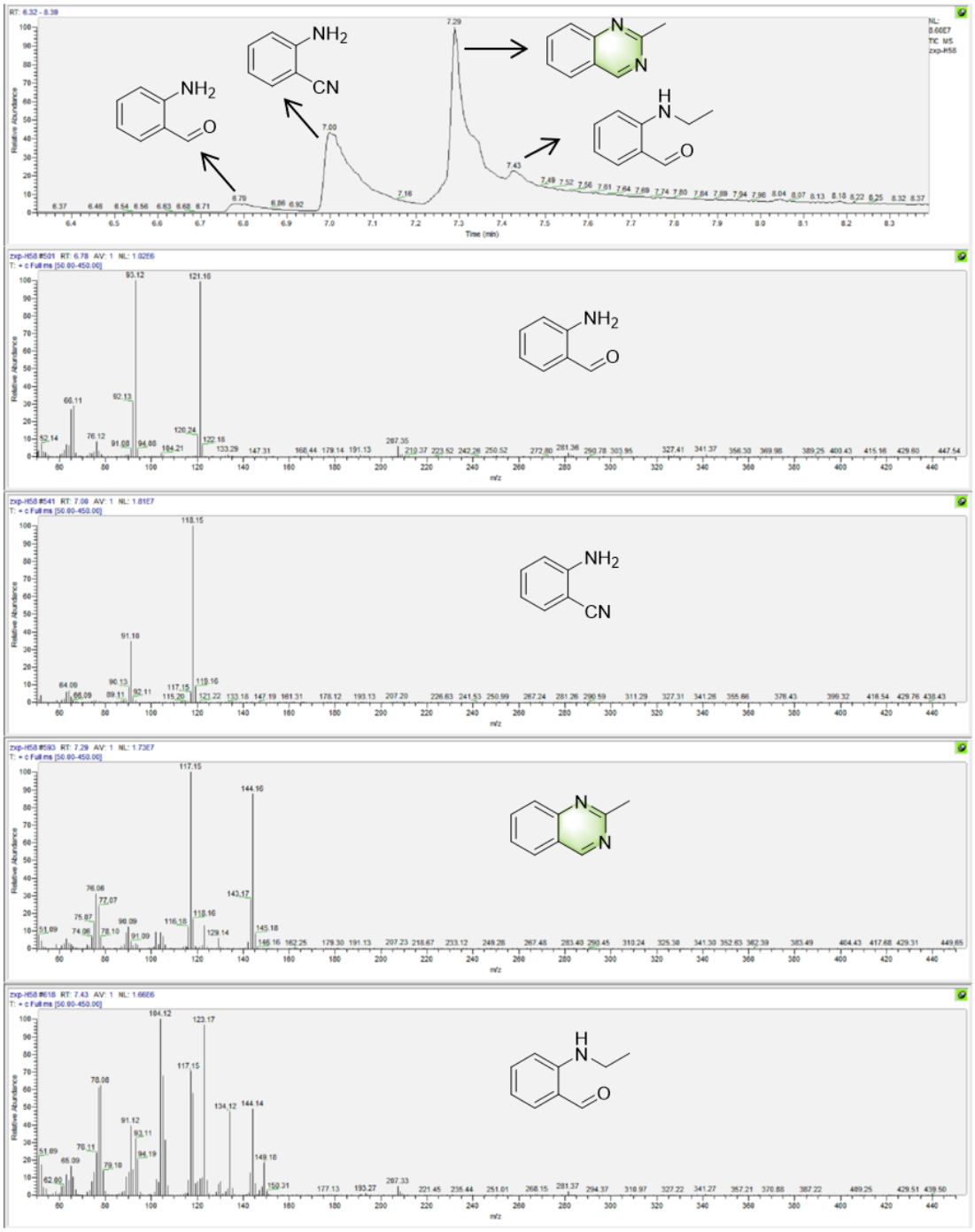

Figure S6 GC-MS spectra of reaction sample.

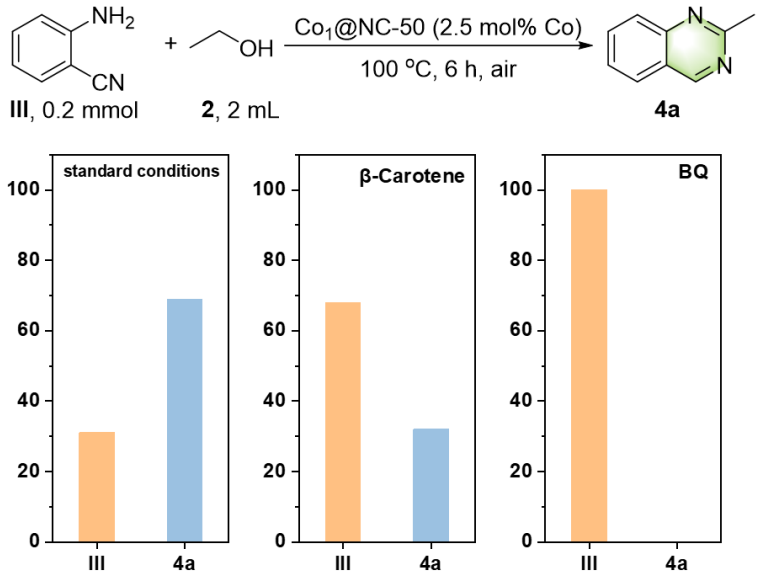

Figure S7 Inhibition experiments.

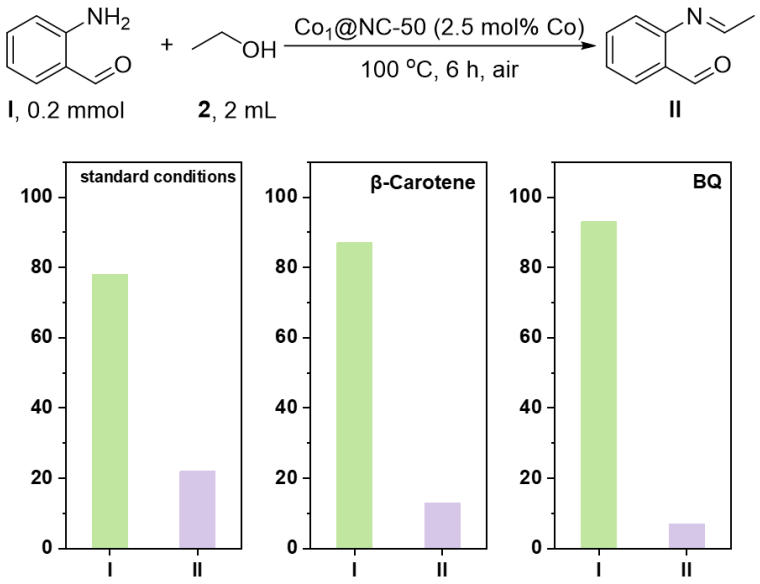

Figure S8 Inhibition experiments.

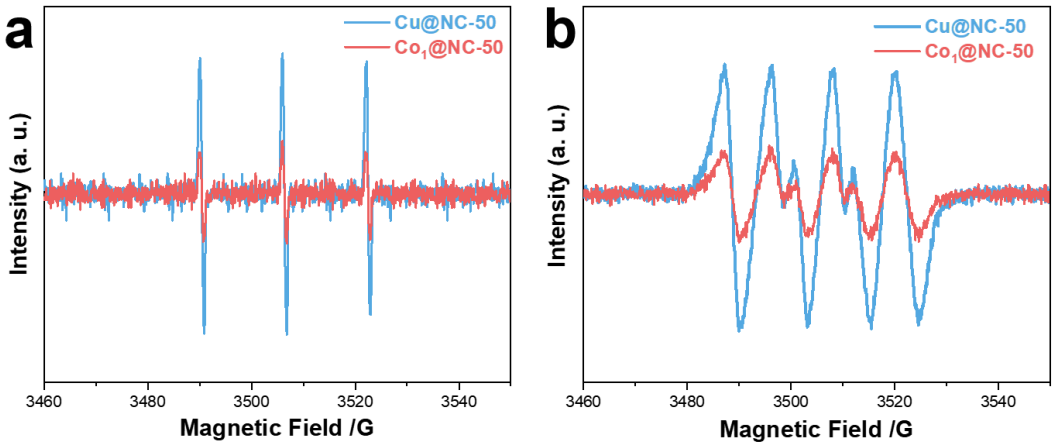

Figure S9 EPR spectra of (a) $^1O_2$ and (b) $\bullet O_2^-$ for Co_1@NC-50 and Cu@NC-50.

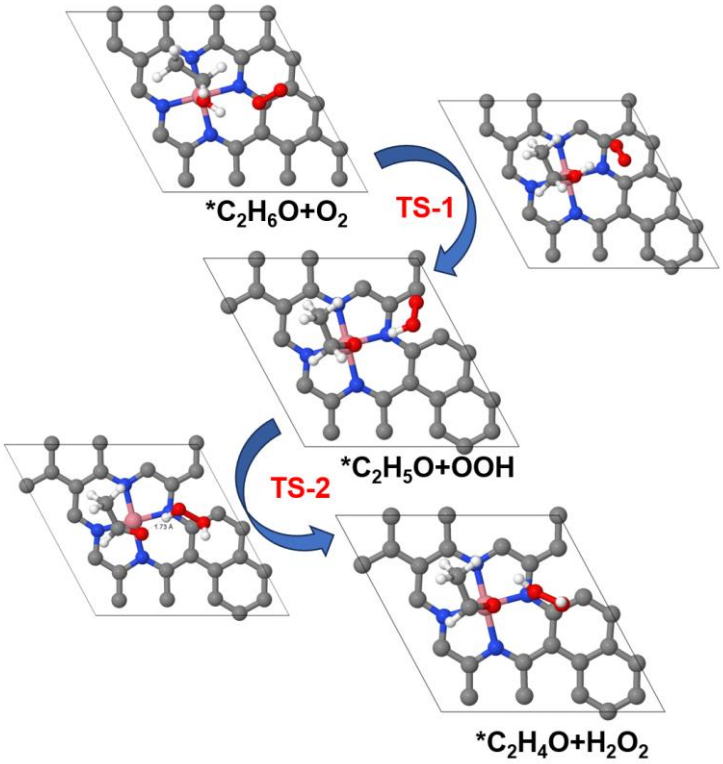

Figure S10 Reaction path of aerobic dehydrogenation for ethanol to acetaldehyde on Co-N_4 site.

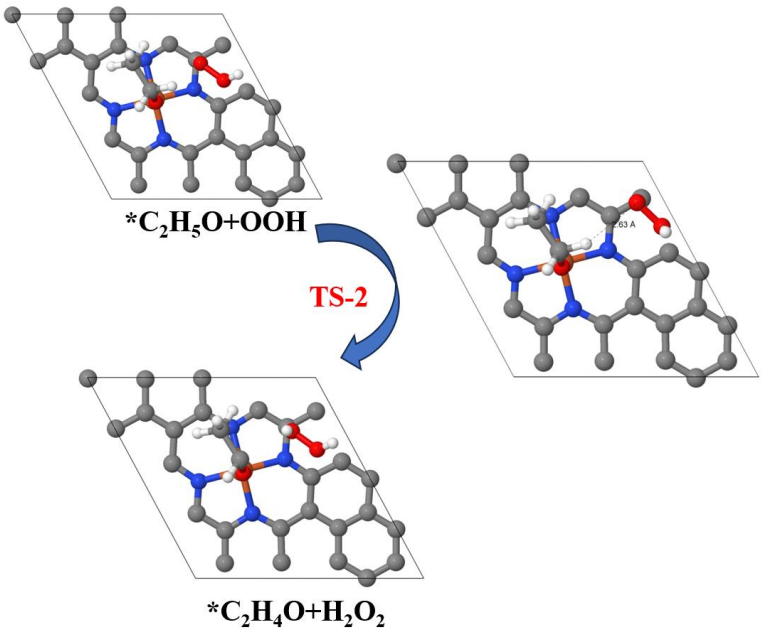

Figure S11 Reaction path of aerobic dehydrogenation for ethanol to acetaldehyde on Fe-N_4 site.

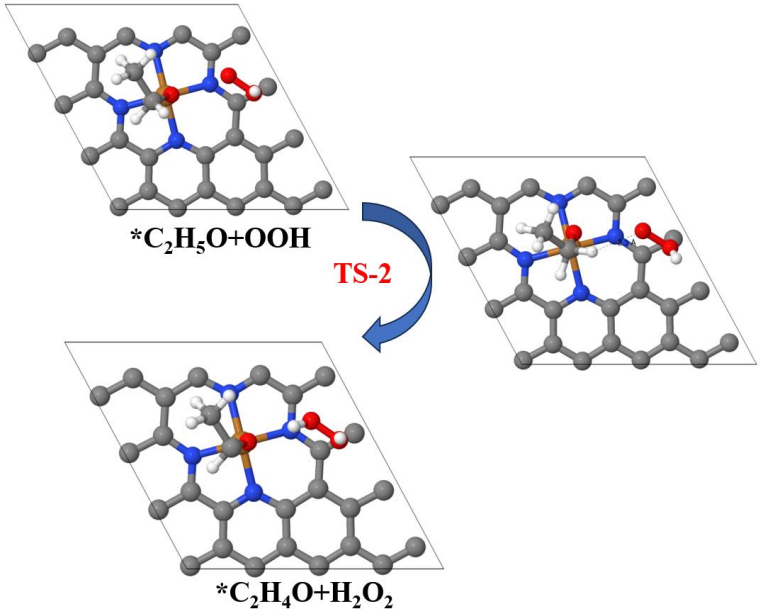

Figure S12 Reaction path of aerobic dehydrogenation for ethanol to acetaldehyde on Cu-N_4 site.

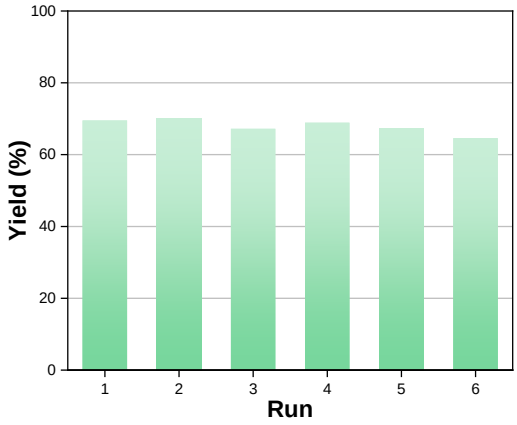

Figure S13 Recycling studies. Reaction conditions: **1a** (0.2 mmol), **2a** (2 mL), **3** (1 mL), Co_1@NC-50 (2.5 mol% Co), Air, 100 °C, 3 h

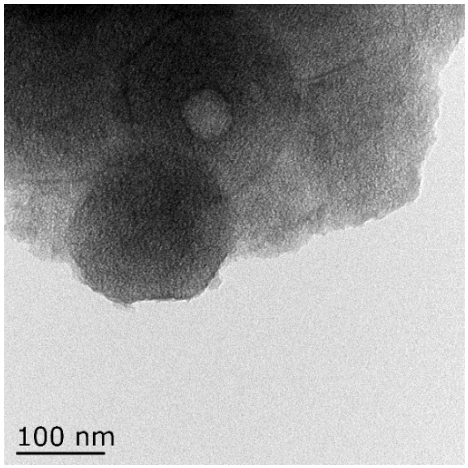

Figure S14 TEM of recycled Co_1@NC-50 after 6 runs.

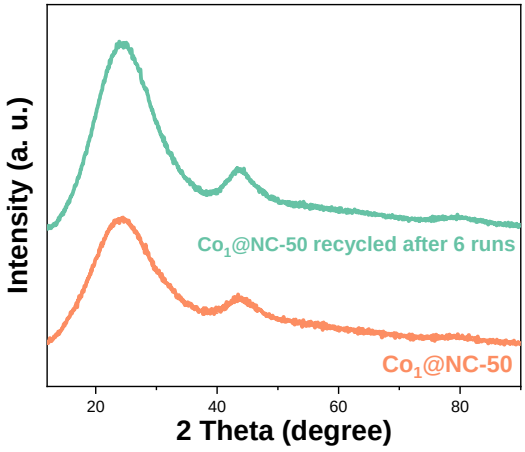

Figure S15 XRD pattern of Co_1@NC-50 and recycled Co_1@NC-50 after 6 runs.

Scheme S1 Gram scale experiment.

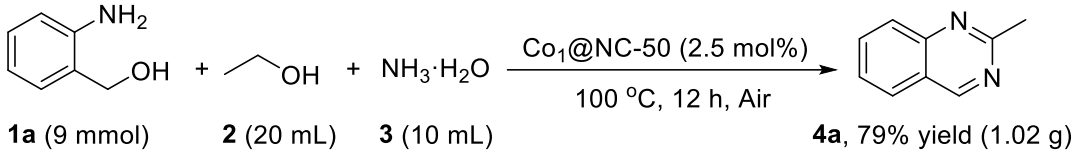

Scheme S2 Control experiments.

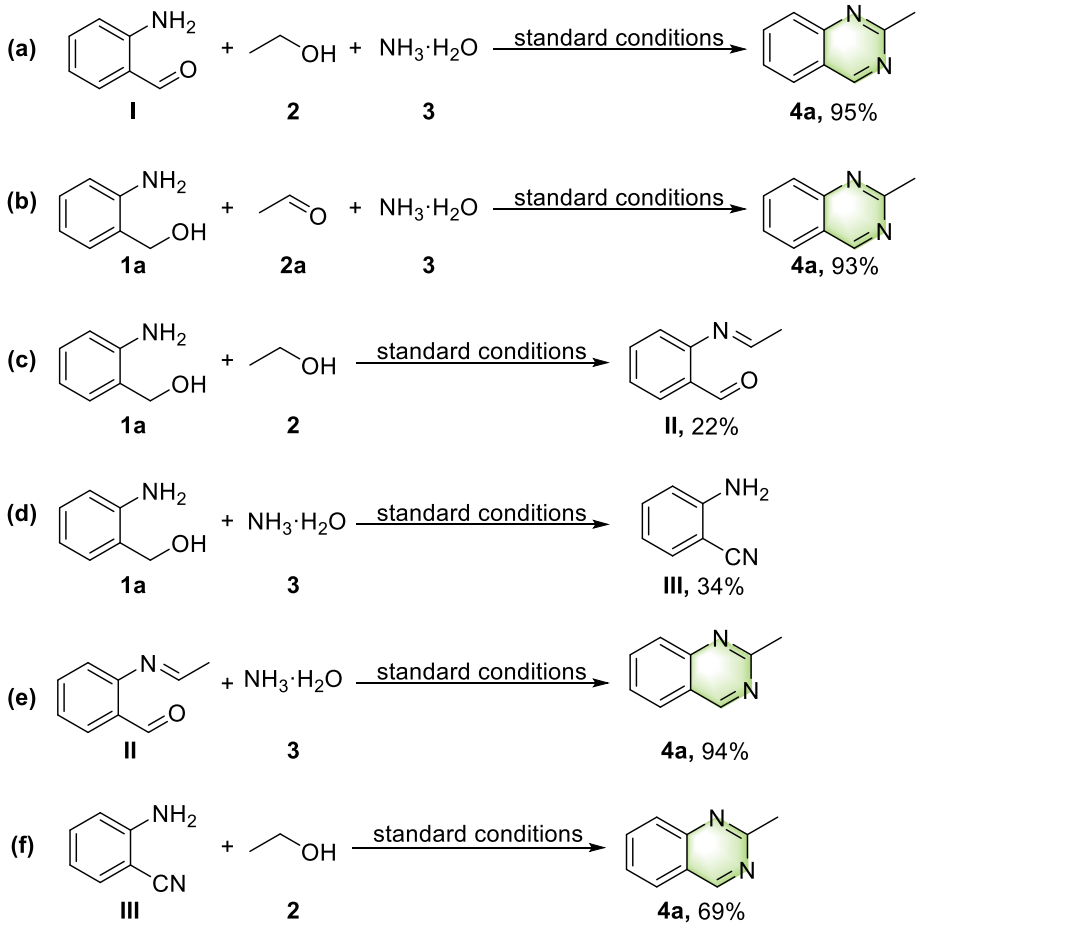

Standard conditions: **I**/**1a**/**II**/**III** (0.2 mmol), **2**/**2a** (2 mL), **3** (1 mL) Co_1@NC-50 (2.5 mol% Co), 100 °C, 6 h, air.

The target product **4a** could be yielded using **I** or **2a** as the starting materials under the standard conditions (**Scheme S2a and S2b**), so **I** and **2a** may be intermediates in the reaction. The produces **II** and **III** could be obtained in the absence ammonia or ethanol, respectively (**Scheme S2c and S2d**). Furthermore, **4a** could be obtained by the reaction of **II** with ammonia, **III** with ethanol, respectively. Those results indicated that

II and **III** may be the intermediates of the reaction (**Scheme S2e and S2f**).

Table S1 ICP results of Co_1@NC-50.

Catalyst	Co content (mg/kg)
Co_1@NC-50	14856.0
Co_1@NC-50 recycled after 6 runs	14561.6

Table S2 The BET surface area and average pore diameter of Co_1@NC-50 and Co@NC-10.

	Co_1@NC-50	Co@NC-10
BET Surface Area (m^2/g)	1115.8	614.6
BJH Adsorption average pore diameter (4V/A) (nm)	2.6	3.8

Table S3 EXAFS data fitting results of Co_1@NC-50.

Sample	Path	*CN*[a]	*R*(Å)[b]	σ^2 (Å^2)[c]	ΔE_0(eV)[d]	*R* factor
Co K-edge (S_0^2=0.744)						
Co foil	Co-Co	12*	2.492±0.001	0.0063	7.6	0.0008
Co-1.5%	Co-N	4.2±0.5	1.882±0.022	0.0064	-10.9	0.0118

[a]*CN*, coordination number; [b]*R*, the distance between absorber and backscatter atoms; [c]σ^2, the Debye Waller factor value; [d]ΔE_0, inner potential correction to account for the difference in the inner potential between the sample and the reference compound; *R* factor indicates the goodness of the fit. $S0^2$ was fixed to 0.744, according to the experimental EXAFS fit of Co foil by fixing *CN* as the known crystallographic value. * This value was fixed during EXAFS fitting, based on the known structure of Co. Fitting conditions: *k* range：3.0 - 11.0; *R* range: 1.0-2.0; fitting space: R space; *k*-weight = 3. A reasonable range of EXAFS fitting parameters: $0.700 < S_0^2 < 1.000$; $CN > 0$; $\sigma^2 > 0$ Å^2; $|\Delta E_0| < 15$ eV; *R* factor < 0.02.

Table S4 Catalytic activity of M@NC-50 (M = Co, Fe, Cu, Mo).[a,b]

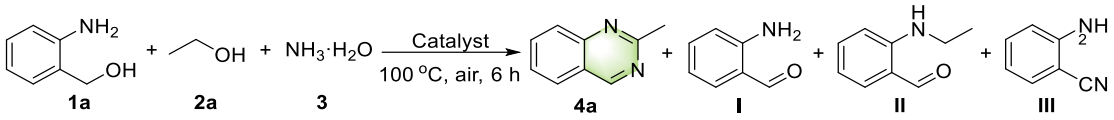

1a 2a 3 4a I II III

Catalyst	Conv. (%)	Yield of **4a**	Yield of **I**	Yield of **II**	Yield of **III**
Co_1@NC-50	97	97	—	—	—
Fe@NC-50	95	48	4	3	40
Cu@NC-50	95	30	1	12	52
Mo@NC-50	67	22	25	14	6
Co@C	23	9	9	2	3
NC	64	24	22	3	15
Co@NC-20	96	86	—	2	8
Co@NC-10	95	48	7	12	28
$Co(NO_3)_2$•$6H_2O$	96	61	10	9	16
$Co(OAc)_2$•$4H_2O$	96	52	21	15	8
CoPc	94	71	5	8	10
$Co(acac)_2$	41	15	3	4	19
Co_2O_3	6	—	6	—	—

[a] Reaction conditions: **1a** (0.2 mmol), **2a** (2 mL), **3** (1 mL), catalyst (M = 2.5 mol%), air, 100 °C, 6 h. [b] Yields were determined by GC using mesitylene as the internal standard.

11. Characterization data

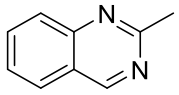

Chemical Formula: $C_9H_8N_2$
Exact Mass: 144.07

2-Methylquinazoline (**4a**), white solid (81%, 23.3 mg). ^{1}H NMR (500 MHz, $CDCl_3$): δ 9.39 (s, 1H), 8.03-8.01 (d, *J* = 8.5 Hz, 1H), 7.96-7.92 (m, 2H), 7.67-7.64 (t, *J* = 15.0 Hz, 1H), 2.97 (s, 3H). GC-MS (EI) *m/z*: 144.

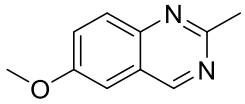

Chemical Formula: $C_{10}H_{10}N_2O$
Exact Mass: 174.08

6-Methoxy-2-methylquinazoline (**4l**), white solid (90%, 31.3 mg). ^{1}H NMR (500 MHz, $CDCl_3$): δ 9.36 (s, 1H), 8.07-8.05 (d, *J* = 9.0 Hz, 1H), 7.66-7.63 (t, *J* = 12.0 Hz, 1H), 7.22 (s, 1H), 4.02 (s, 3H), 2.99 (s, 3H). GC-MS (EI) *m/z*: 174.

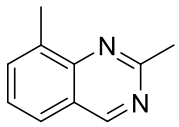

Chemical Formula: $C_{10}H_{10}N_2$
Exact Mass: 158.08

2,8-Dimethylquinazoline (**4m**), white solid (91%, 28.8 mg). ^{1}H NMR (500 MHz, $CDCl_3$): δ 9.33 (s, 1H), 7.77-7.76 (d, *J* = 7.5 Hz, 2H), 7.54-7.51 (t, *J* = 15 Hz, 1H), 2.97 (s, 3H), 2.81 (s, 3H). ^{13}C NMR (125 MHz, $CDCl_3$): δ 163.42, 160.18, 149.63, 136.28, 134.01, 126.59, 124.91, 122.77, 26.53, 16.98. GC-MS (EI) *m/z*: 158.

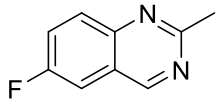

Chemical Formula: $C_9H_7FN_2$
Exact Mass: 162.06

6-Fluoro-2-methylquinazoline (**4n**), white solid (77%, 24.9 mg). ^{1}H NMR (500 MHz, $CDCl_3$): δ 9.37 (s, 1H), 8.07-8.04 (m, 1H), 7.74-7.70 (m, 1H), 7.58-7.56 (dd, *J* = 10.5 Hz, 1H), 2.96 (s, 3H). GC-MS (EI) *m/z*: 162.

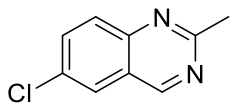

Chemical Formula: $C_9H_7ClN_2$
Exact Mass: 178.03

6-Chloro-2-methylquinazoline (**4o**), white solid (81%, 28.8 mg). ^{1}H NMR (500 MHz, $CDCl_3$): δ 9.32 (s, 1H), 7.97-7.93 (m, 2H), 7.87-7.85 (t, *J* = 11.0 Hz, 1H), 2.95 (s, 3H). ^{13}C NMR (125 MHz, $CDCl_3$): δ 164.93, 159.42, 148.84, 135.14, 132.60, 129.56, 125.80, 123.35, 26.39. GC-MS (EI) *m/z*: 178.

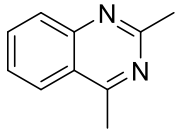

Chemical Formula: $C_{10}H_{10}N_2$
Exact Mass: 158.08

2,4-Dimethylquinazoline (**4q**), white solid (91%, 28.8 mg). ^{1}H NMR (500 MHz, $CDCl_3$): δ 8.13-8.12 (d, *J* = 8.5 Hz, 1H), 8.03-8.01 (d, *J* = 8.0 Hz, 1H), 7.92-7.90 (m, 1H), 7.65-7.62 (t, *J* = 15.5 Hz, 1H), 3.00 (s, 3H), 2.92 (s, 3H). GC-MS (EI) *m/z*: 158.

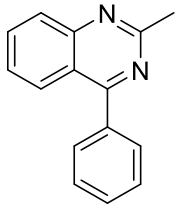

Chemical Formula: $C_{15}H_{12}N_2$
Exact Mass: 220.10

2-Methyl-4-phenylquinazoline (**6a**), white solid (90%, 39.6 mg). ^{1}H NMR (500 MHz, $CDCl_3$): δ 8.10-8.05 (m, 2H), 7.93-7.89 (m, 1H), 7.80-7.78 (t, *J* = 8.5 Hz 1H), 7.61-7.56 (m, 4H), 3.00-2.99 (d, *J* = 5.5 Hz, 3H). ^{13}C NMR (125 MHz, $CDCl_3$): δ 168.66, 163.87, 151.44, 137.32, 133.69, 129.89, 128.67, 128.65, 128.15, 127.08, 126.77, 121.08, 26.61, 1.05. GC-MS (EI) *m/z*: 220.

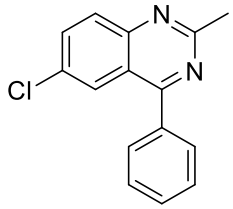

Chemical Formula: $C_{15}H_{11}ClN_2$
Exact Mass: 254.06

6-Chloro-2-methyl-4-phenylquinazoline (**6b**), white solid (91%, 46.2 mg). ^{1}H NMR (500 MHz, $CDCl_3$): δ 8.06-8.05 (d, *J* = 2.5 Hz, 1H), 8.01-8.00 (d, *J* = 9.0 Hz, 1H), 7.84-7.82 (dd, 1H), 7.78-7.77 (m, 2H), 7.63-6.62 (t, *J* = 6.5 Hz, 3H), 2.98 (s, 3H). ^{13}C NMR (125 MHz, $CDCl_3$): δ 167.83, 164.21, 149.91, 136.75, 134.58, 132.41, 130.20, 129.93, 129.83, 129.78, 128.86, 128.84, 125.77, 121.60, 26.54. GC-MS (EI) *m/z*: 254.

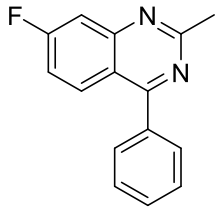

Chemical Formula: $C_{15}H_{11}FN_2$
Exact Mass: 238.09

7-Fluoro-2-methyl-4-phenylquinazoline (**6c**), white solid (89%, 42.4 mg). ^{1}H NMR (500 MHz, $CDCl_3$): δ 8.08-8.06 (t, *J* = 14.0 Hz, 2H), 7.94-7.91 (t, *J* = 15.5 Hz, 1H),

7.83-7.80 (dd, 2H), 7.61-7.58 (t, J = 15.0 Hz, 1H), 7.33-7.29 (t, J = 17.5 Hz, 2H), 2.99 (s, 3H). ^{13}C NMR (125 MHz, $CDCl_3$): δ 167.52, 164.95, 163.81, 162.96, 151.40, 133.82, 133.39, 131.93, 128.22, 126.95, 126.74, 120.95, 115.89, 115.72, 26.53. GC-MS (EI) *m/z*: 238.

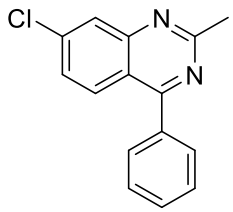

Chemical Formula: $C_{15}H_{11}ClN_2$
Exact Mass: 254.06

7-Chloro-2-methyl-4-phenylquinazoline (**6d**), white solid (89%, 45.2 mg). ^{1}H NMR (500 MHz, $CDCl_3$): δ 8.07-8.03 (m, 2H), 7.93-7.90 (t, J = 15.0 Hz, 1H), 7.76-7.74 (d, J = 8.5 Hz, 2H), 7.60-7.56 (m, 3H), 2.98 (s, 3H). GC-MS (EI) *m/z*: 254.

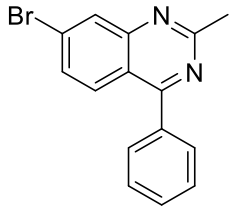

Chemical Formula: $C_{15}H_{11}BrN_2$
Exact Mass: 298.01

7-Bromo-2-methyl-4-phenylquinazoline (**6e**), white solid (90%, 53.6 mg). ^{1}H NMR (500 MHz, $CDCl_3$): δ 8.08-8.04 (dd, 2H), 7.94-7.91 (t, J = 16.5 Hz, 1H), 7.77-7.75 (d, J = 8.5 Hz, 2H), 7.70-7.68 (d, J = 8.5 Hz, 2H), 7.60-7.57 (t, J = 15.5 Hz, 1H), 2.99 (s, 3H). GC-MS (EI) *m/z*: 298.

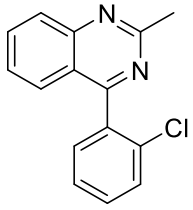

Chemical Formula: $C_{15}H_{11}ClN_2$
Exact Mass: 254.06

4-(2-Chlorophenyl)-2-methyl-phenylquinazoline (**6g**), white solid (84%, 42.7 mg). ^{1}H NMR (500 MHz, $CDCl_3$): δ 8.05-8.03 (d, J = 8.5 Hz, 1H), 7.89-7.86 (t, J = 15.5 Hz, 1H), 7.61-7.55 (dd, 2H), 7.52-7.44 (m, 4H), 2.97 (s, 3H). ^{13}C NMR (125 MHz, $CDCl_3$): δ 167.32, 163.92, 150.83, 136.21, 134.08, 132.80, 130.80, 130.66, 129.99, 128.05, 127.06, 127.02, 126.87, 121.64, 29.73, 26.54. GC-MS (EI) *m/z*: 254.

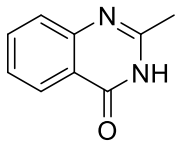

Chemical Formula: $C_9H_8N_2O$
Exact Mass: 160.06

2-Methylquinazolin-4(3H)-one (**8a**), white solid (72%, 23.0 mg). ^{1}H NMR (500 MHz, DMSO-d6): δ 12.18 (brs, 1H), 8.07-8.06 (d, *J* = 7.5 Hz, 1H), 7.77-7.73 (m, 1H), 7.57-7.55 (d, *J* = 8.0 Hz, 1H), 7.45-7.42 (t, *J* = 16.0 Hz, 1H), 2.34 (s, 3H). ^{13}C NMR (125 MHz, DMSO-d6): δ 162.19, 154.72, 149.42, 134.69, 127.02, 126.28, 126.13, 121.09, 21.90. GC-MS (EI) *m/z*: 160.

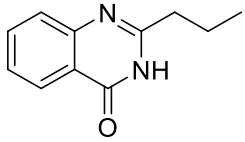

Chemical Formula: $C_{11}H_{12}N_2O$
Exact Mass: 188.09

2-Propyl-4(3*H*)-quinazolinone (**8d**), white solid (64%, 24.1 mg). ^{1}H NMR (500 MHz, $CDCl_3$): δ 11.12 (brs, 1H), 8.29-8.27 (d, *J* = 8.0 Hz, 1H), 7.78-7.69 (m, 2H), 7.48-7.45 (t, *J* = 15.0 Hz, 1H), 2.77-2.74 (t, *J* = 15.5 Hz, 2H), 1.95-1.87 (m, 2H), 1.09-1.06 (t, *J* = 15.0 Hz, 3H). ^{13}C NMR (125 MHz, $CDCl_3$): δ 163.77, 156.44, 149.38, 134.81, 127.24, 126.42, 126.29, 120.60, 37.82, 29.71, 20.95, 13.72. GC-MS (EI) *m/z*: 188.

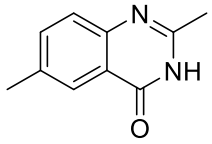

Chemical Formula: $C_{10}H_{10}N_2O$
Exact Mass: 174.08

2,6-Dimethylquinazolin-4(3H)-one (**8e**), white solid (77%, 26.8 mg). ^{1}H NMR (500 MHz, DMSO-d6): δ 12.09 (brs, 1H), 7.86 (s, 1H), 7.59-7.57 (d, *J* = 10.0 Hz, 1H), 7.47-7.46 (d, *J* = 8.5 Hz, 1H), 2.41 (s, 3H), 2.33 (s, 3H). ^{13}C NMR (125 MHz, DMSO-d6): δ 162.13, 153.80, 147.37, 135.97, 135.83, 126.84, 125.50, 120.82, 21.79, 21.19. GC-MS (EI) *m/z*: 174.

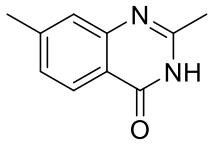

Chemical Formula: $C_{10}H_{10}N_2O$
Exact Mass: 174.08

2,7-Dimethylquinazolin-4(3H)-one (**8f**), white solid (76%, 26.5 mg). ^{1}H NMR (500 MHz, DMSO-d6): δ 11.59 (brs, 1H), 8.12 (s, 1H), 7.63 (s, 2H), 2.63 (s, 3H), 2.55 (s,

3H). GC-MS (EI) *m/z*: 174.

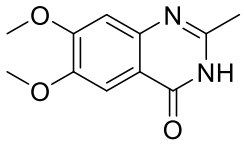

Chemical Formula: $C_{11}H_{12}N_2O_3$
Exact Mass: 220.08

6,7-Dimethoxy-2-methylquinazolin-4(3H)-one (**8g**), white solid (75%, 33.0 mg). ^{1}H NMR (500 MHz, DMSO-d6): δ 11.44 (brs, 1H), 7.58 (s, 1H), 7.10 (s, 1H), 4.02-4.00 (d, *J* = 7.5 Hz, 6H), 2.57 (s, 3H). GC-MS (EI) *m/z*: 220.

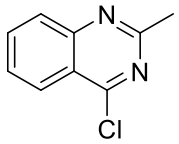

Chemical Formula: $C_9H_7ClN_2$
Exact Mass: 178.03

4-Chloro-2-methylquinazoline (**8aa**), white solid (61%, 54.3 mg). ^{1}H NMR (500 MHz, DMSO-d_6): δ 8.12-8.10 (d, *J* = 8.0 Hz, 1H), 7.92-7.89 (t, *J* = 15.5 Hz, 1H), 7.79-7.77 (d, *J* = 8.0 Hz, 1H), 7.62-7.59 (t, *J* = 15.0 Hz, 1H), 2.56 (s, 3H). GC-MS (EI) *m/z*: 178.

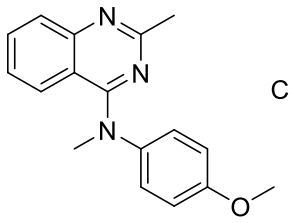

Chemical Formula: $C_{17}H_{17}N_3O$
Exact Mass: 279.14

Verubulin (**8ab**), white solid (63%, 87.9 mg). ^{1}H NMR (500 MHz, DMSO-d6): δ 7.74-7.72 (d, *J* = 8.0 Hz, 1H), 7.53-7.50 (t, *J* = 15.5 Hz, 1H), 7.12-7.10 (d, *J* = 9.0 Hz, 1H), 7.02-6.96 (m, 2H), 6.91-6.89 (d, *J* = 9.0 Hz, 2H), 3.83 (s, 3H), 3.58 (s, 3H), 2.72 (s, 3H). ^{13}C NMR (125 MHz, DMSO-d6): δ 163.37, 161.67, 157.98, 152.17, 141.61, 131.67, 127.67, 127.30, 126.22, 123.94, 115.21, 114.72, 55.53, 42.66, 26.51. GC-MS (EI) *m/z*: 279.

12. ^{1}H and ^{13}C NMR Spectra

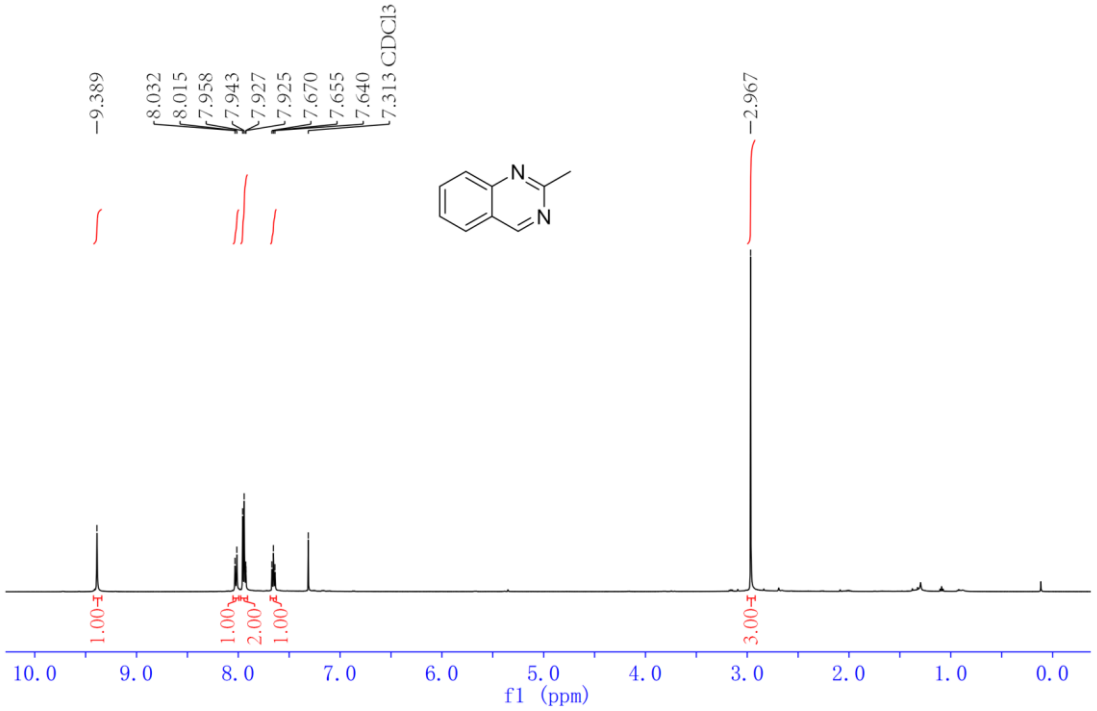

The ^{1}H NMR spectra of **4a**

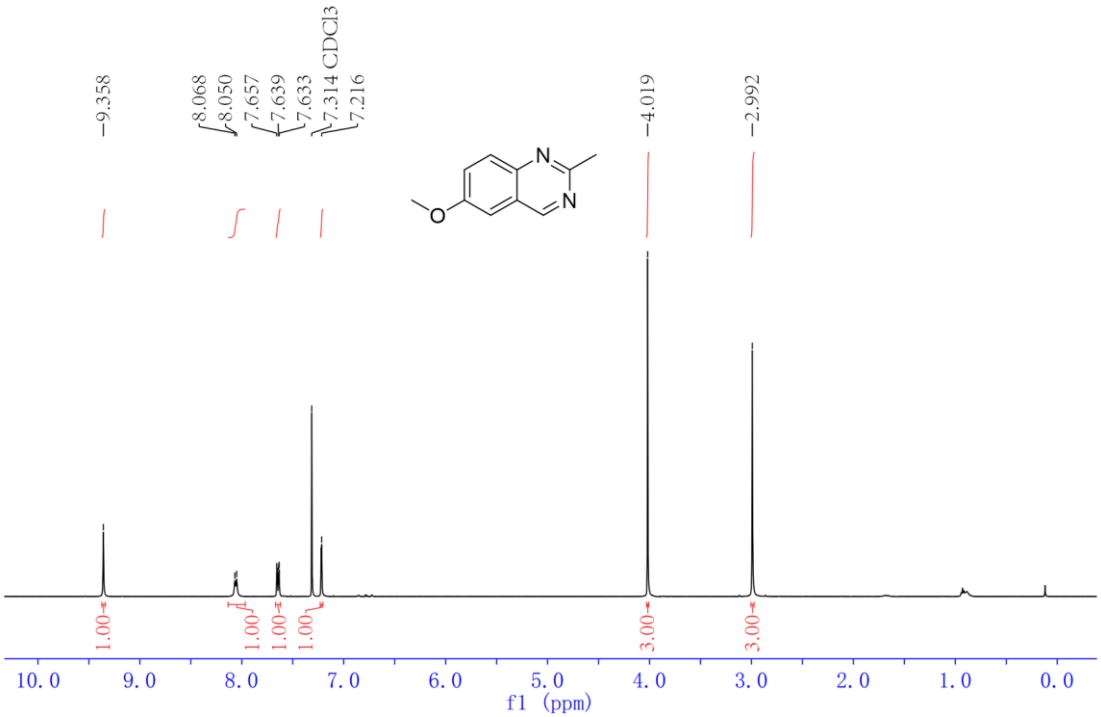

The ^{1}H NMR spectra of **4l**

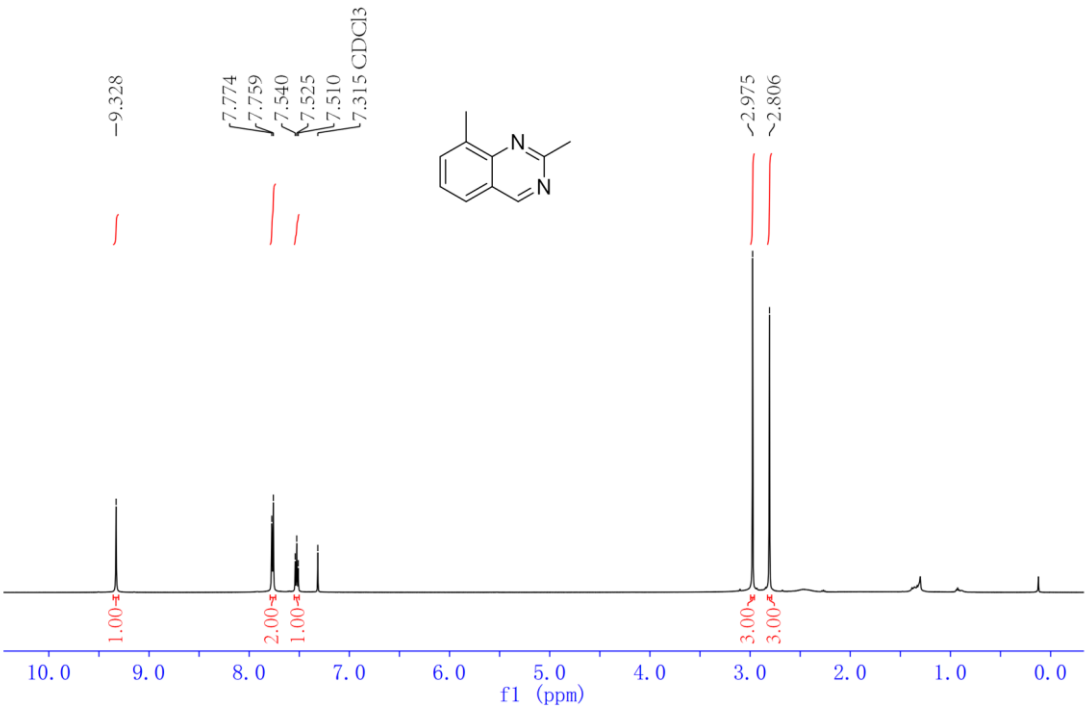

The ^{1}H NMR spectra of **4m**

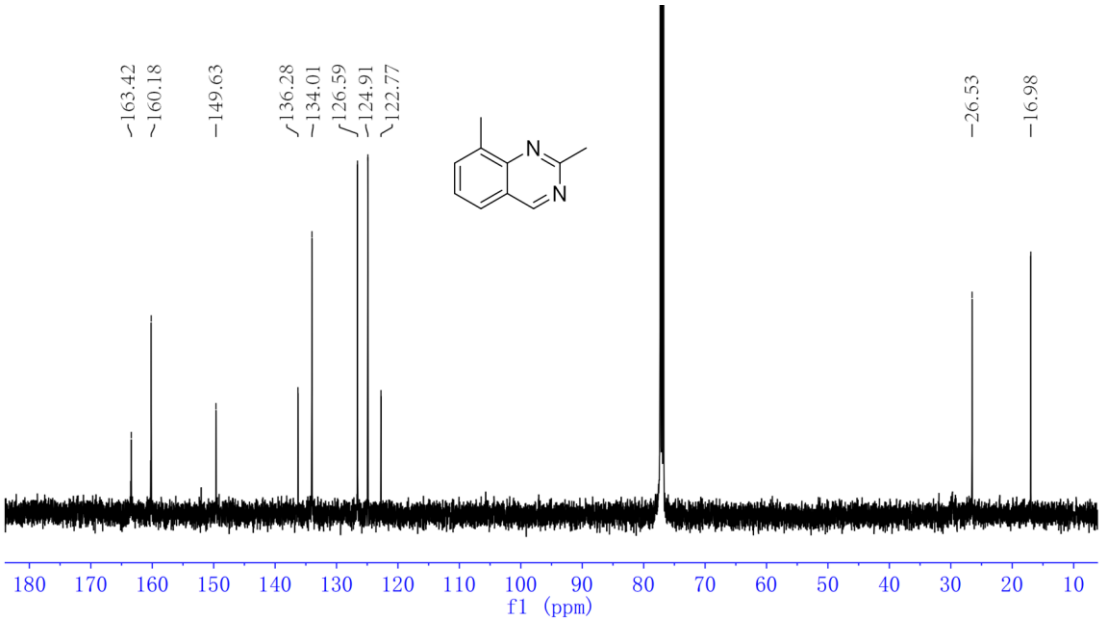

The ^{13}C NMR spectra of **4m**

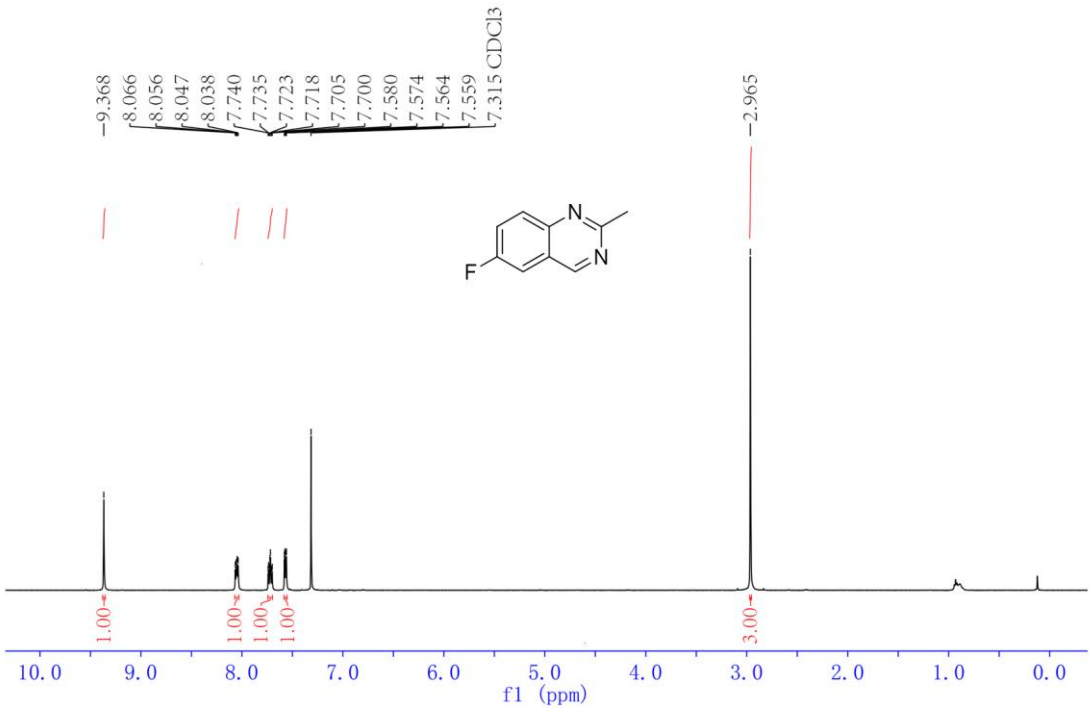

The ^{1}H NMR spectra of **4n**

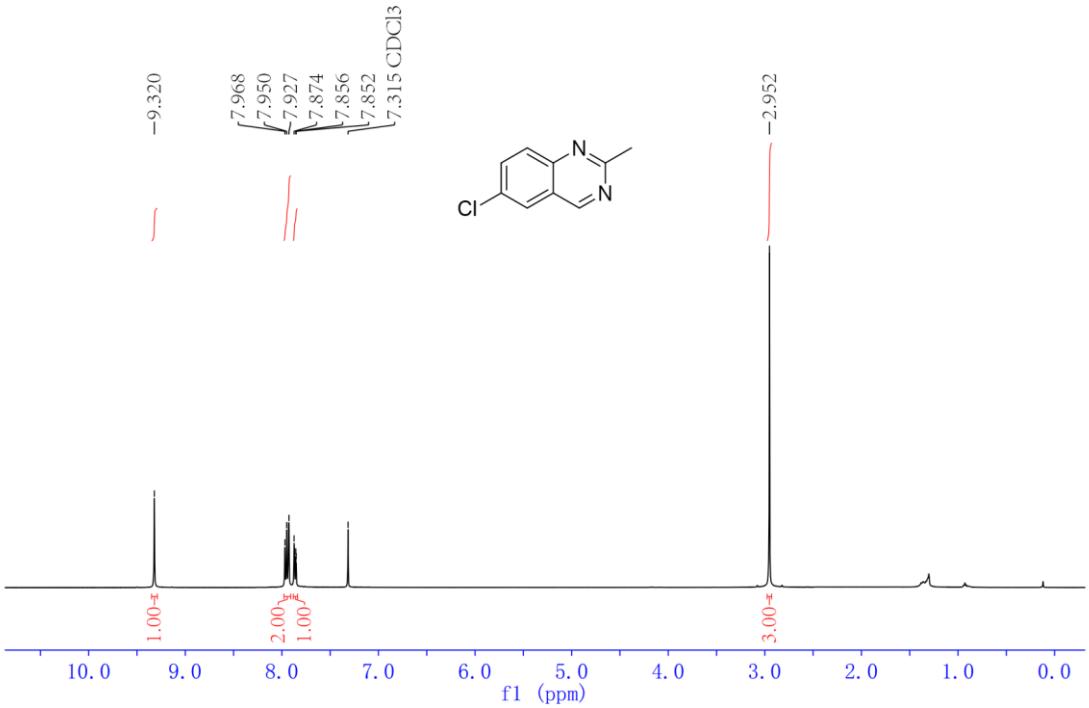

The ^{1}H NMR spectra of **4o**

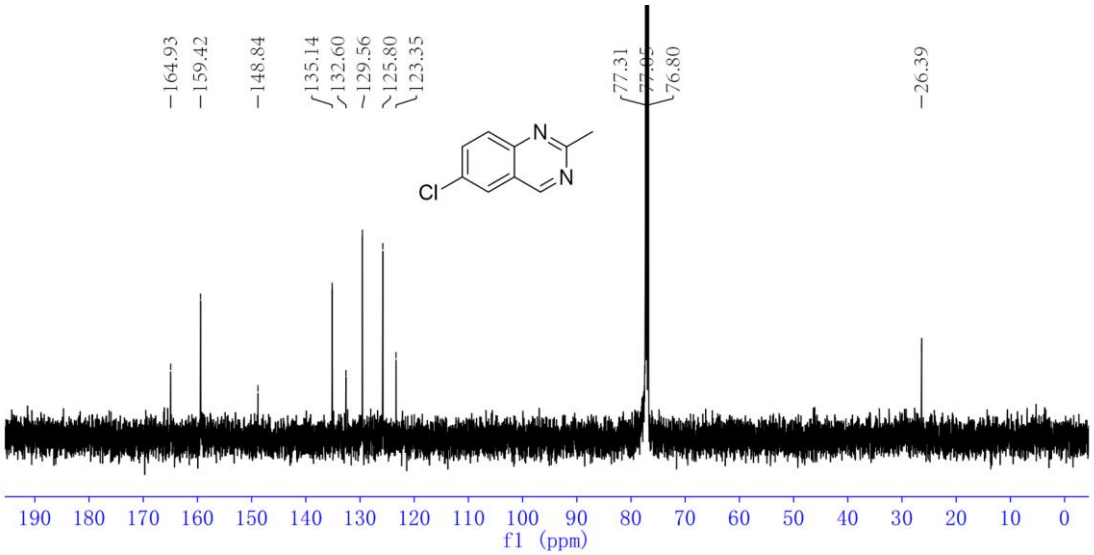

The ^{13}C NMR spectra of **4o**

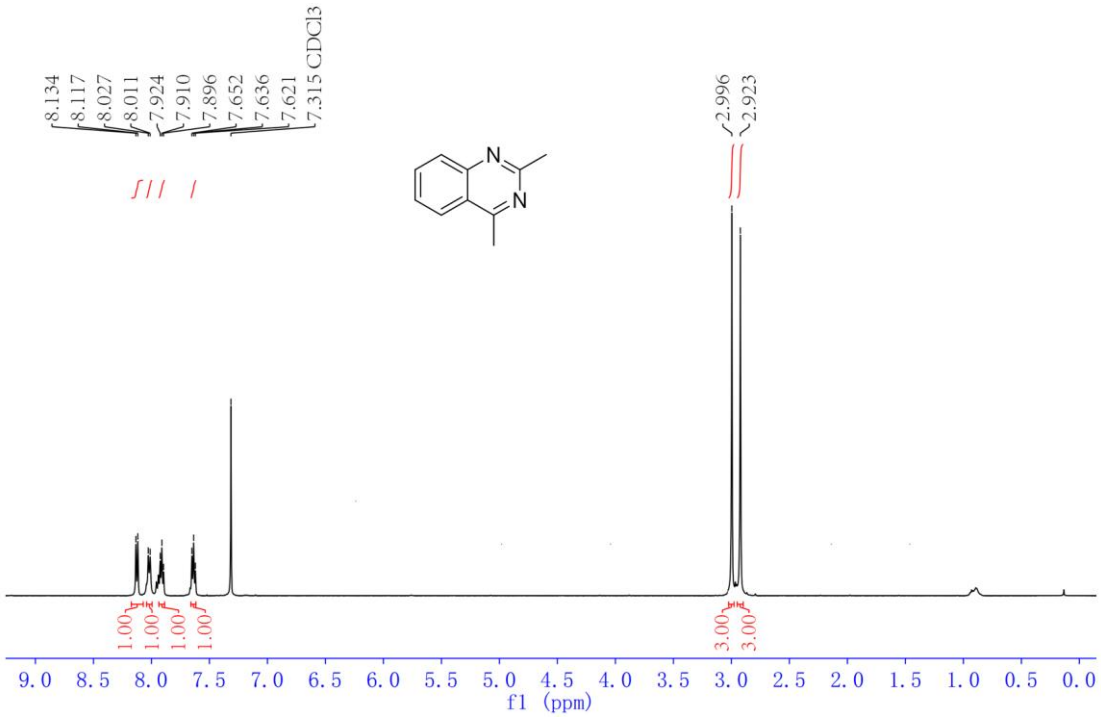

The ^{1}H NMR spectra of **4q**

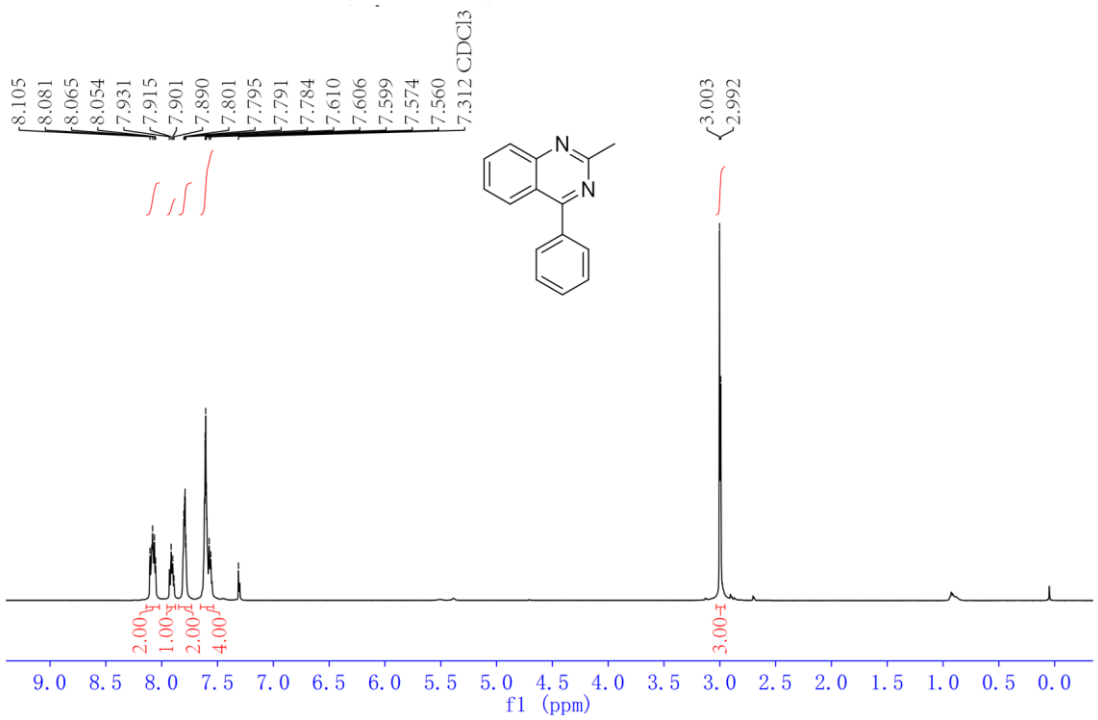

The ^{1}H NMR spectra of **6a**

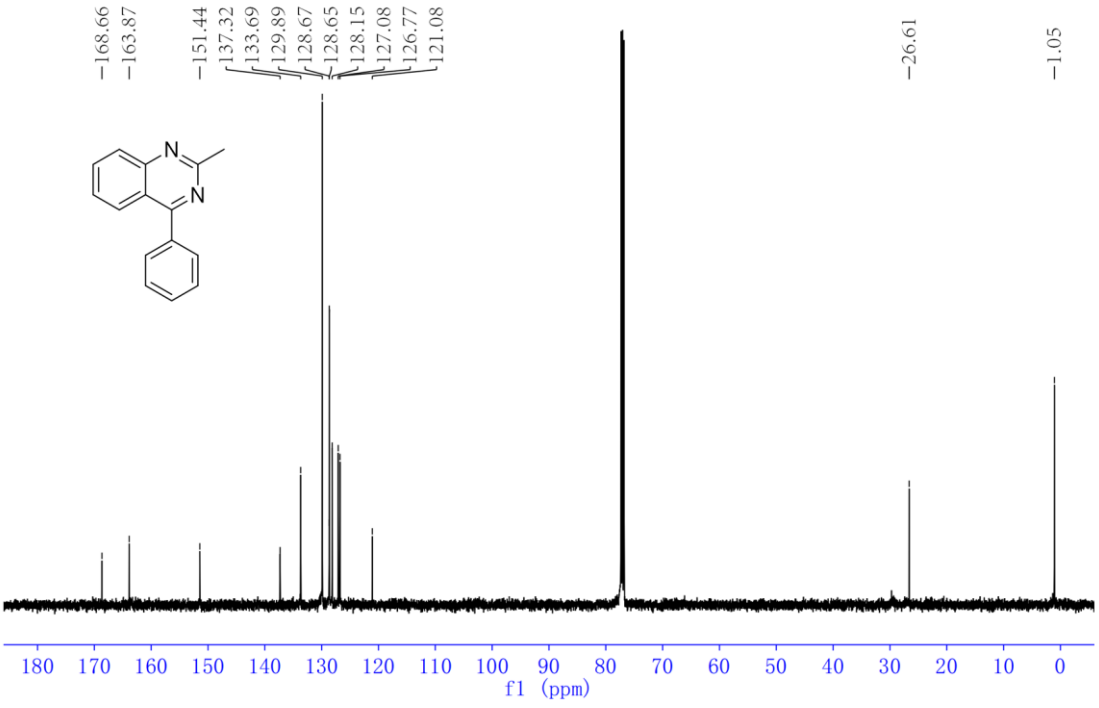

The ^{13}C NMR spectra of **6a**

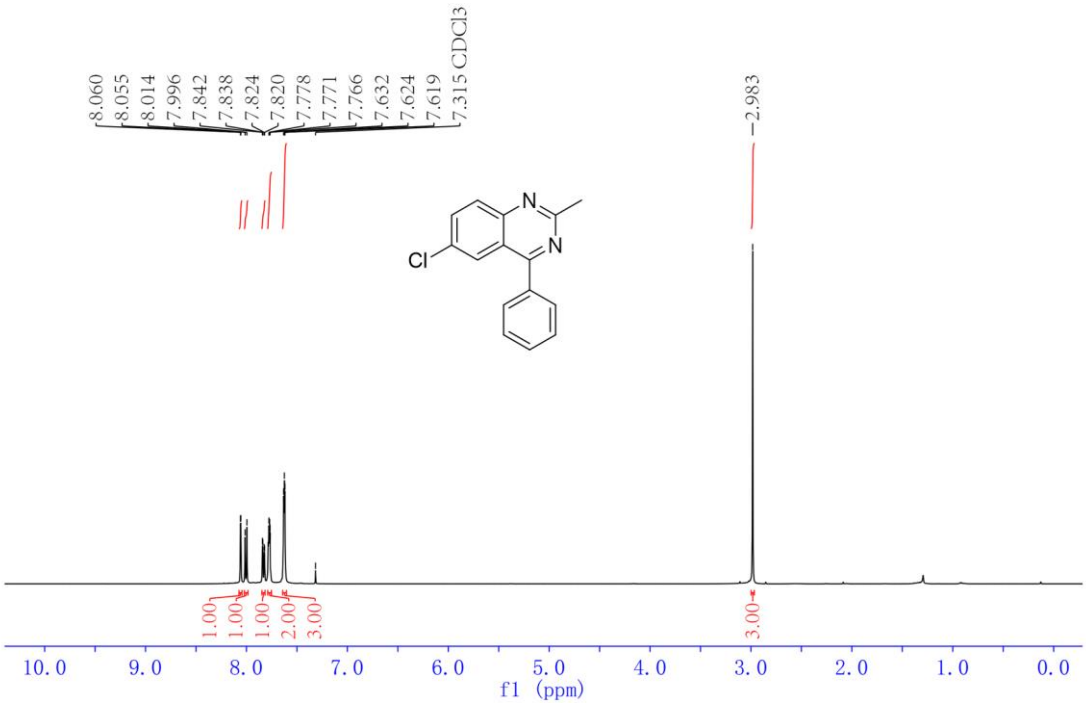

The ^{1}H NMR spectra of **6b**

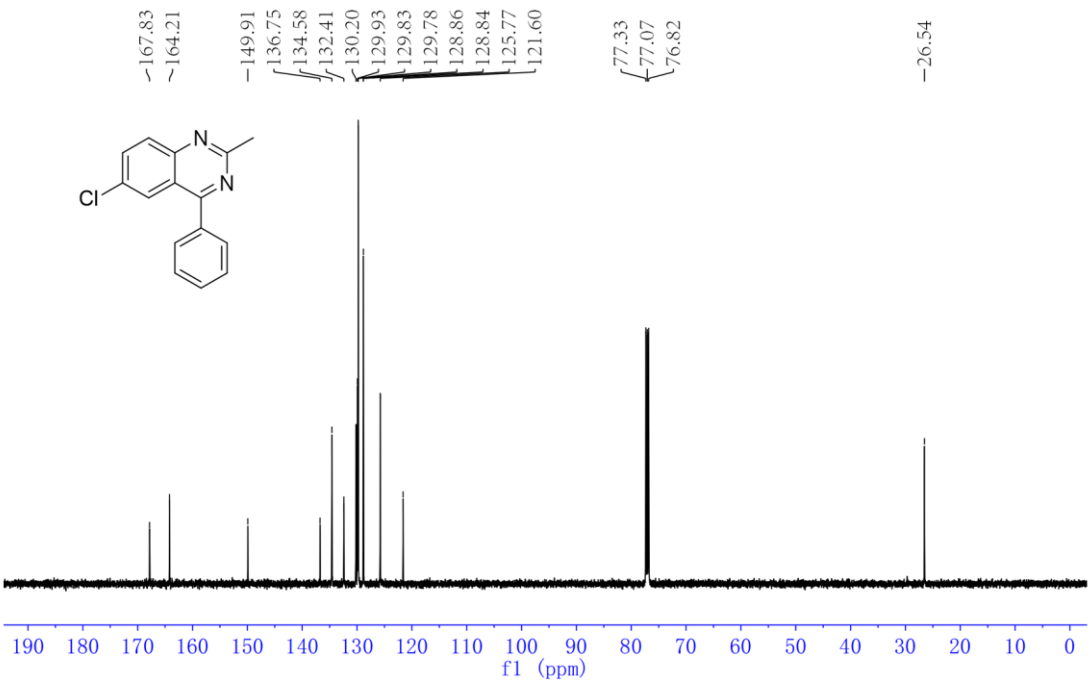

The ^{13}C NMR spectra of **6b**

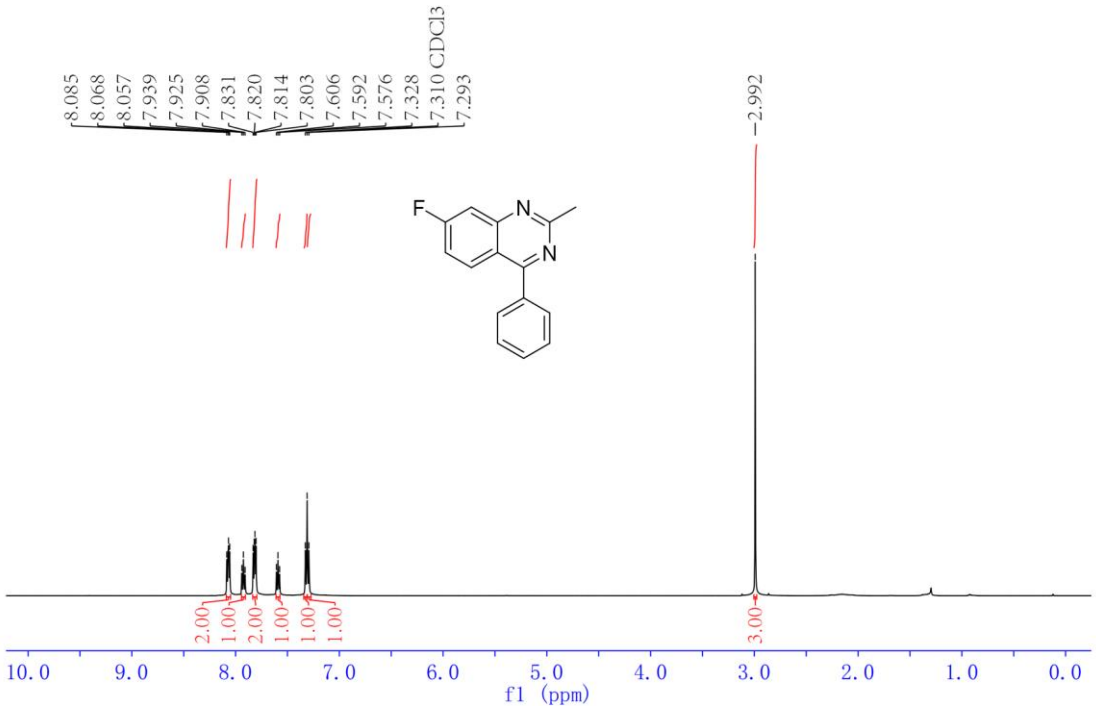

The ^{1}H NMR spectra of **6c**

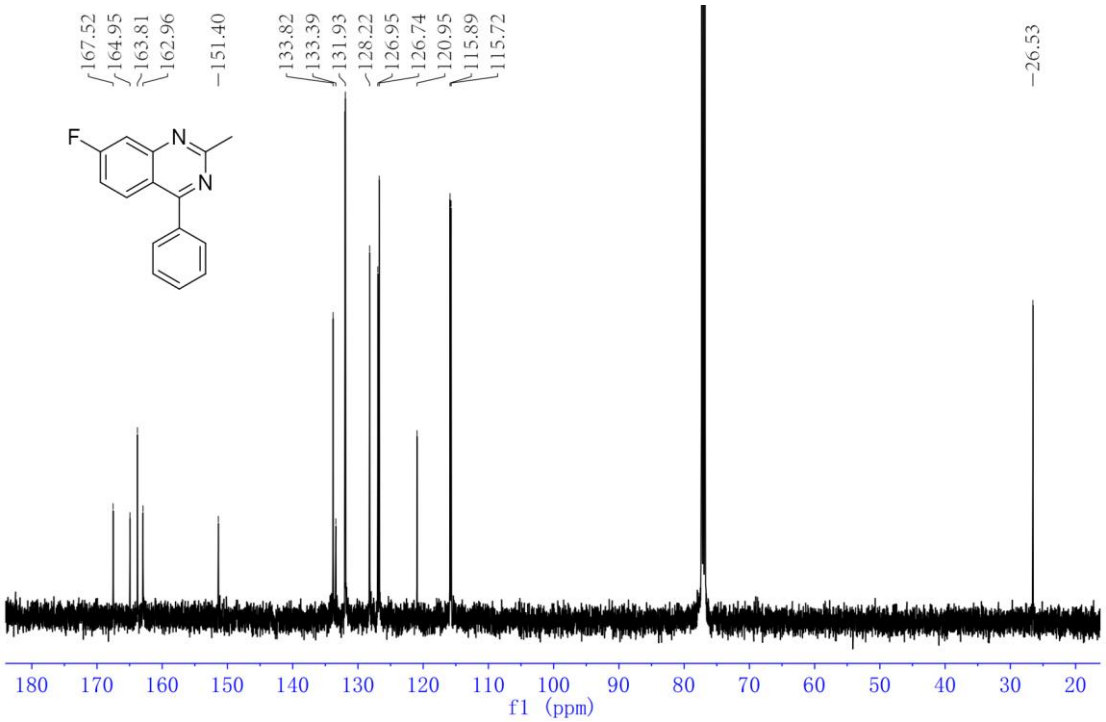

The ^{13}C NMR spectra of **6c**

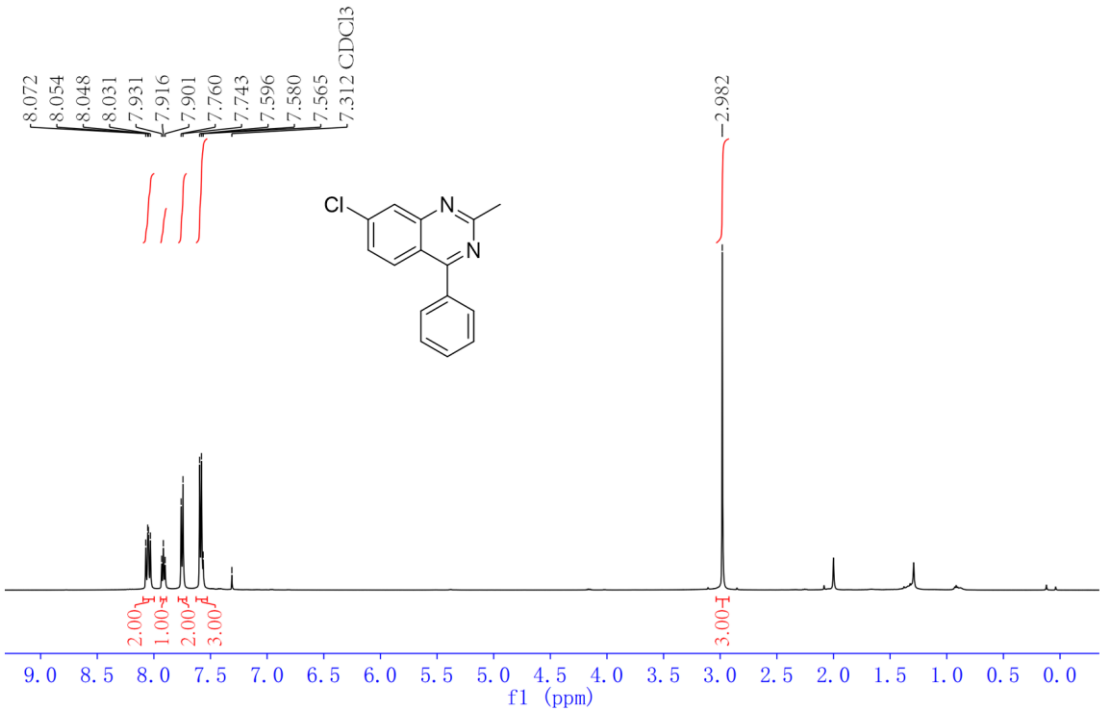

The ^{1}H NMR spectra of **6d**

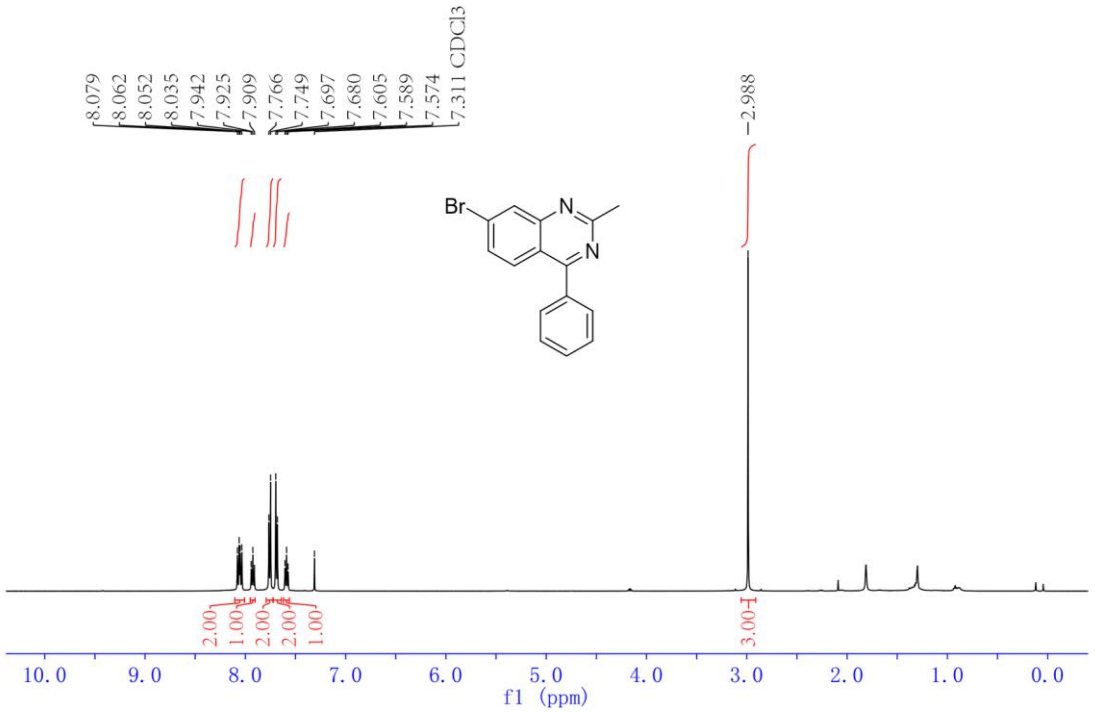

The ^{1}H NMR spectra of **6e**

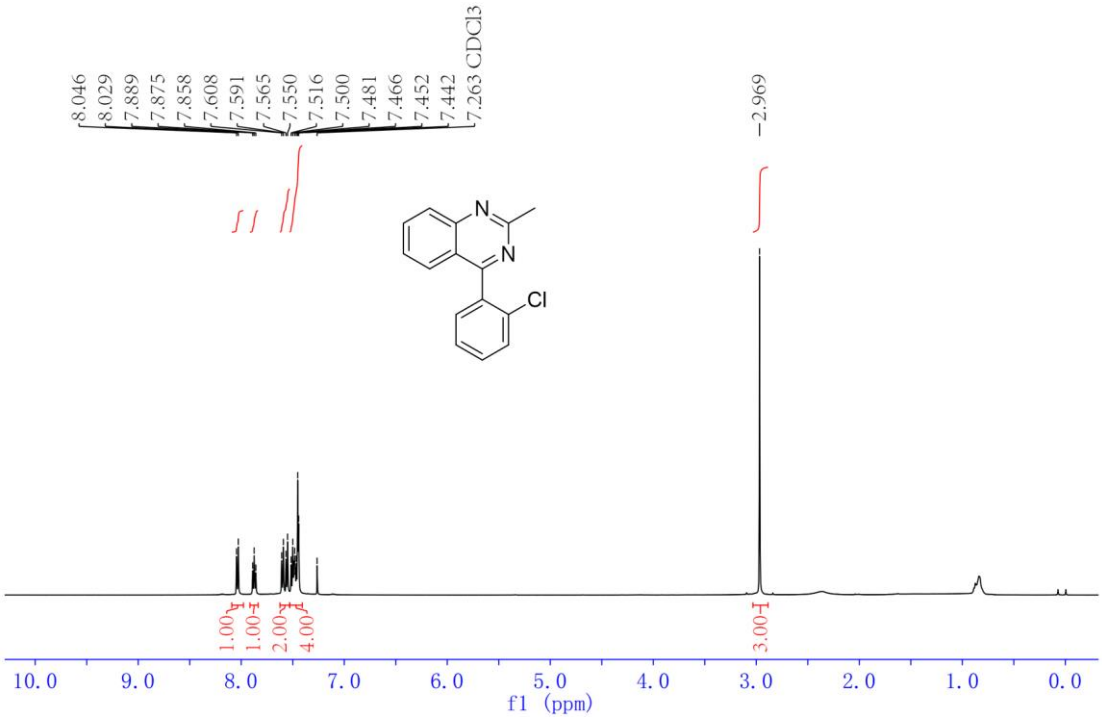

The ^{1}H NMR spectra of **6g**

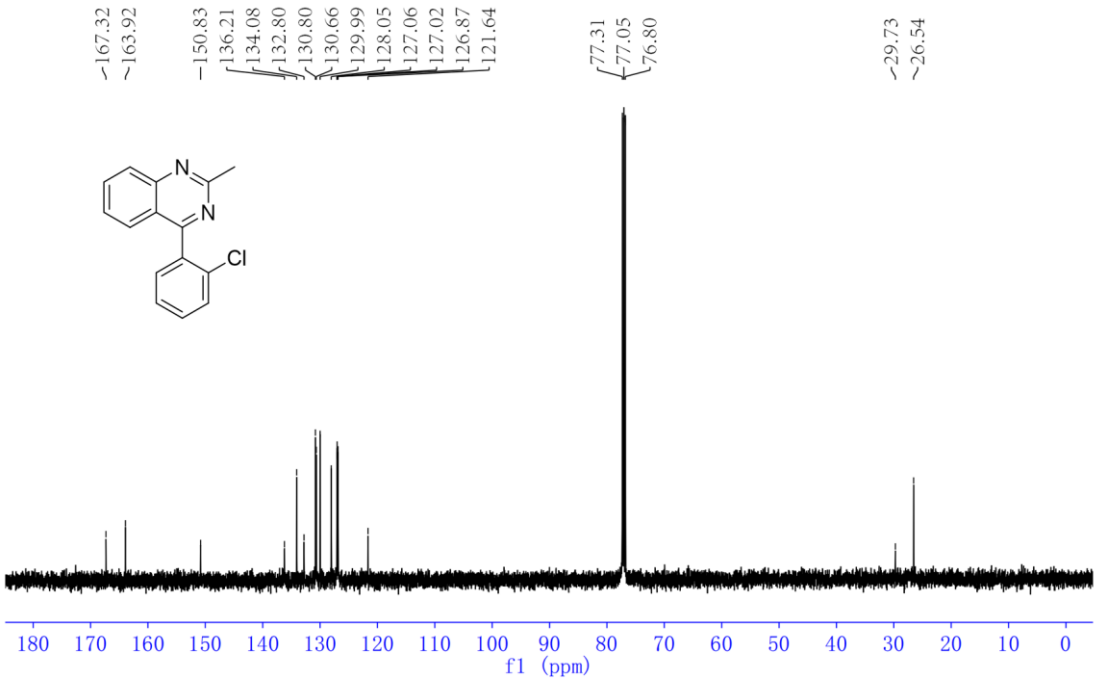

The ^{13}C NMR spectra of **6g**

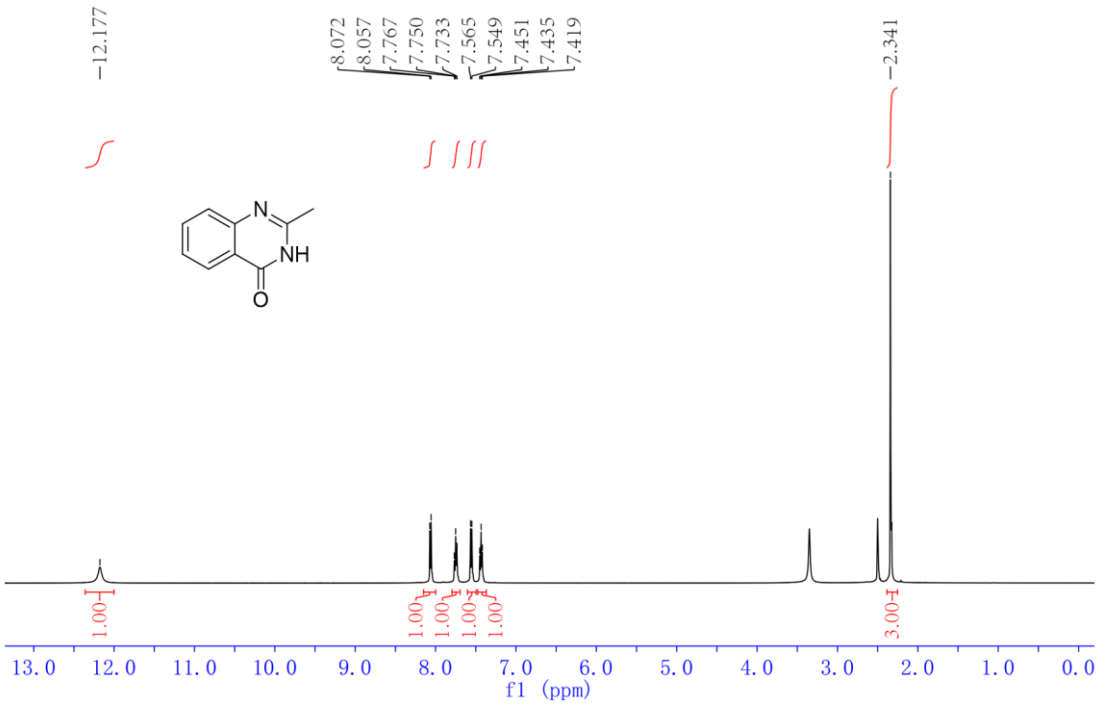

The ^{1}H NMR spectra of **8a**

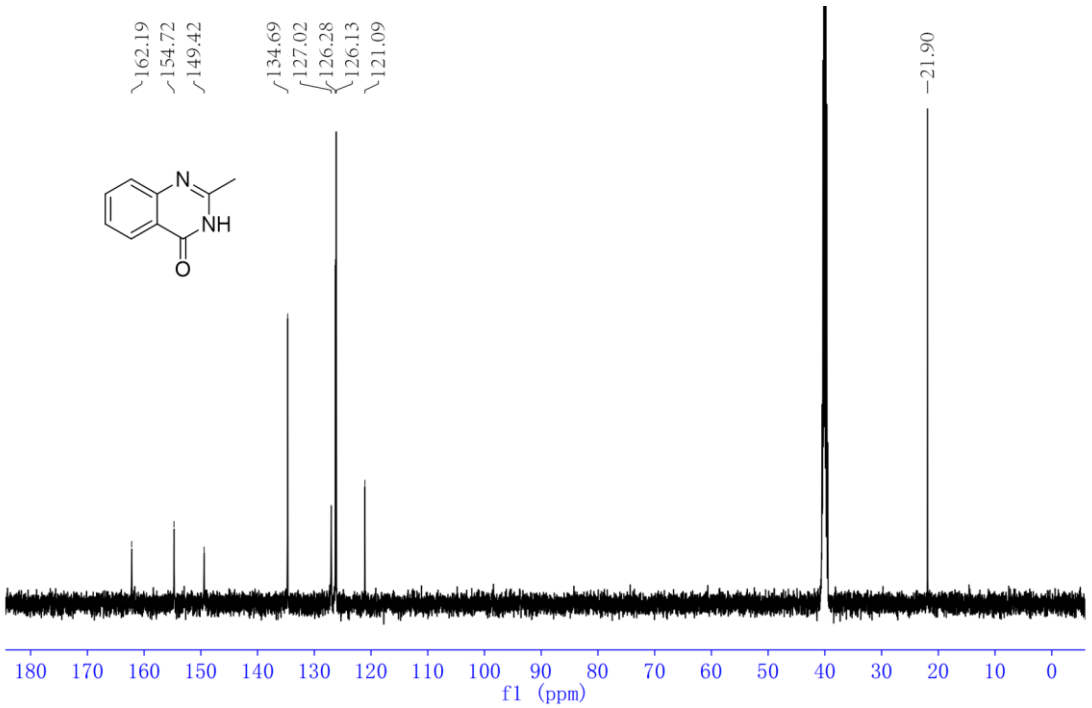

The ^{13}C NMR spectra of **8a**

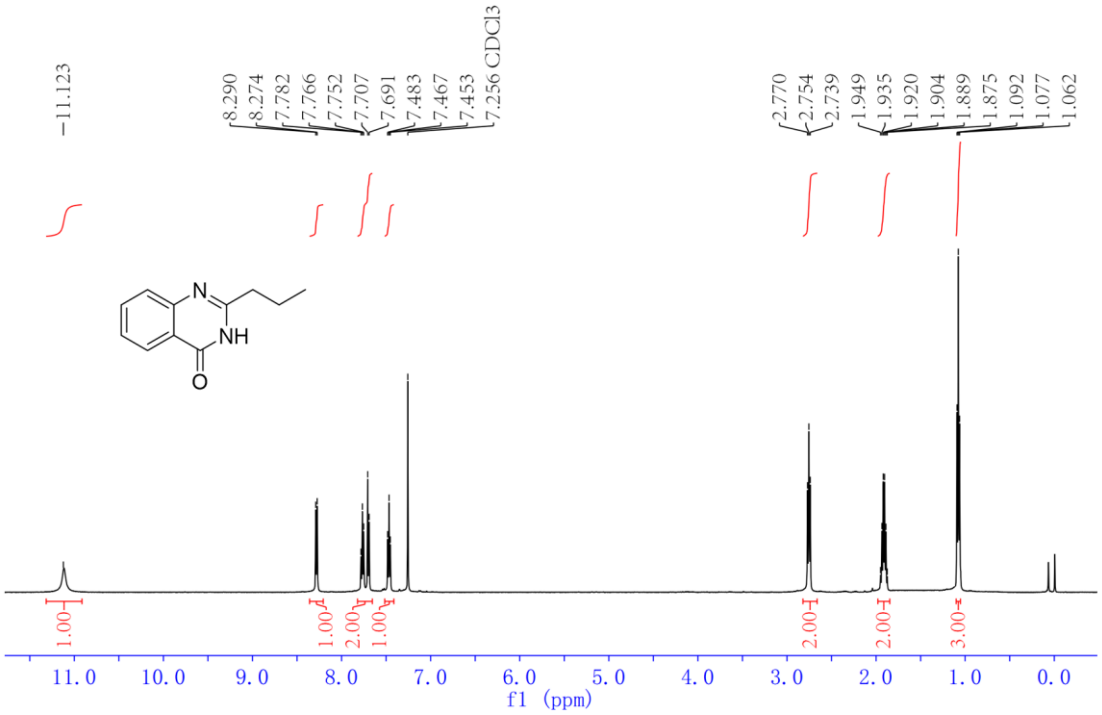

The ^{1}H NMR spectra of **8d**

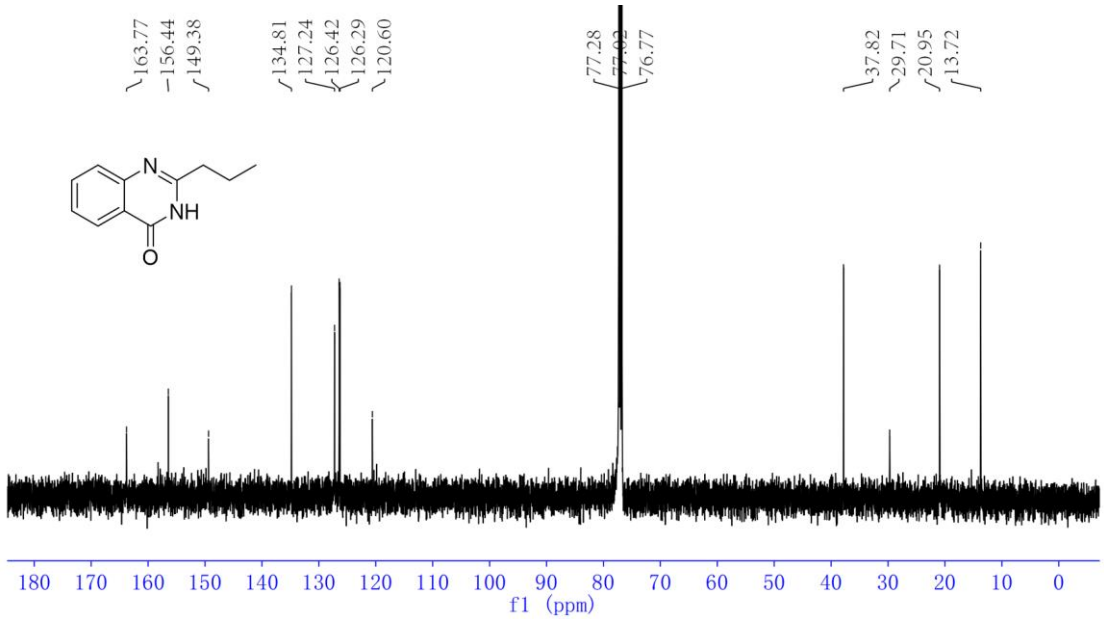

The ^{13}C NMR spectra of **8d**

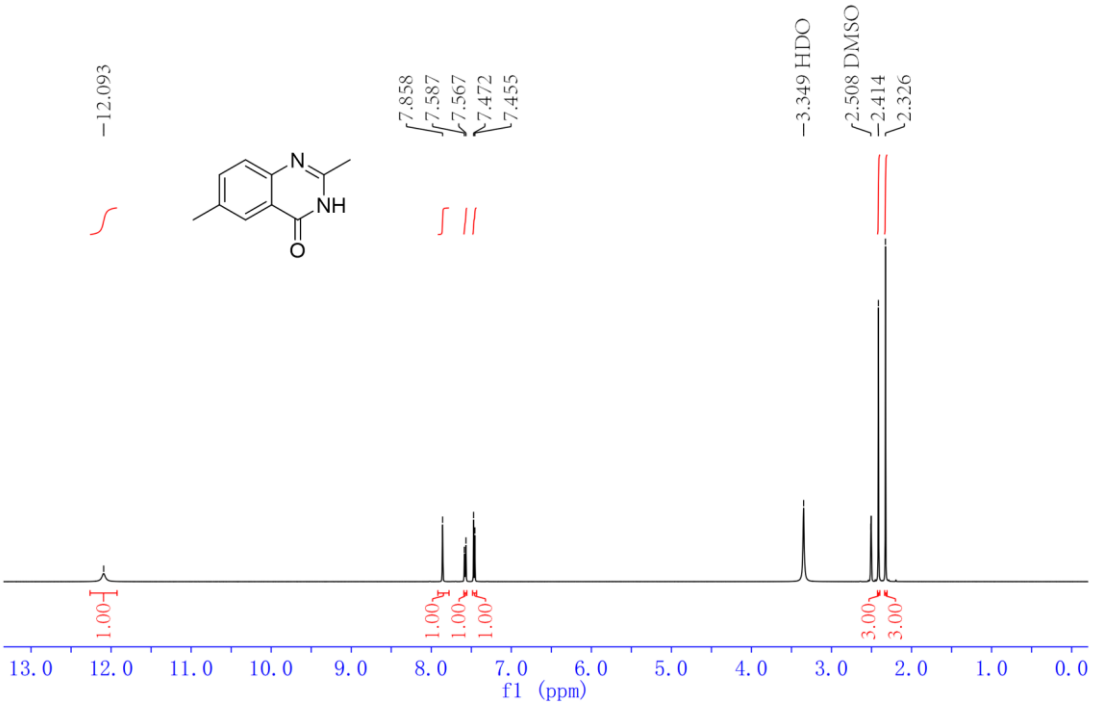

The ^{1}H NMR spectra of **8e**

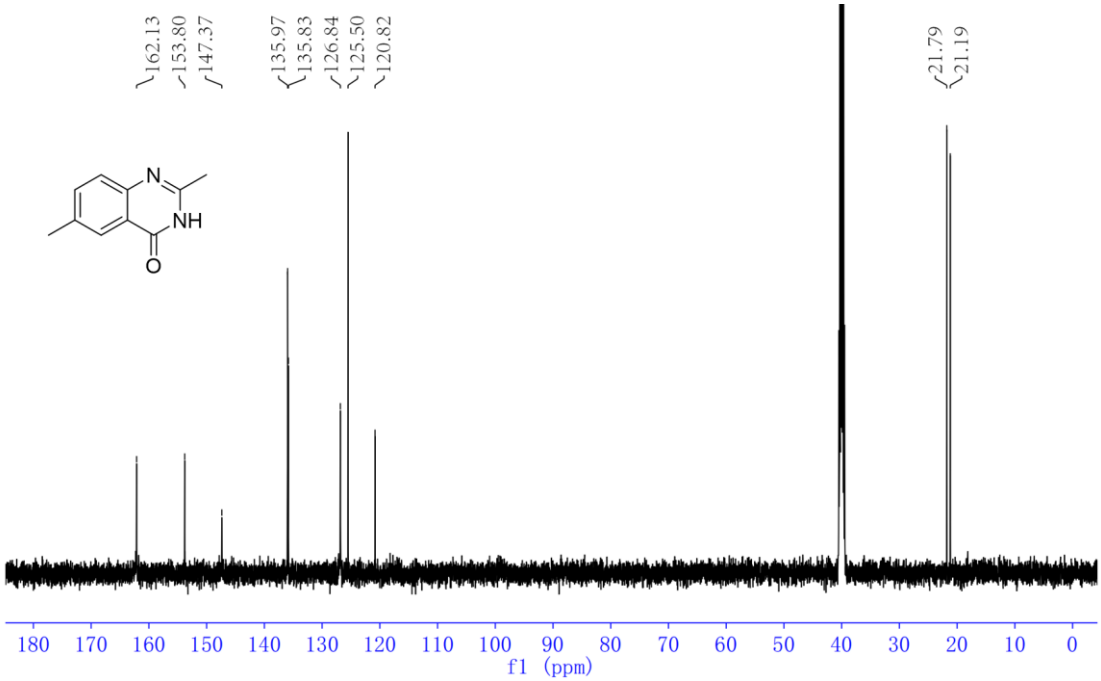

The ^{13}C NMR spectra of **8e**

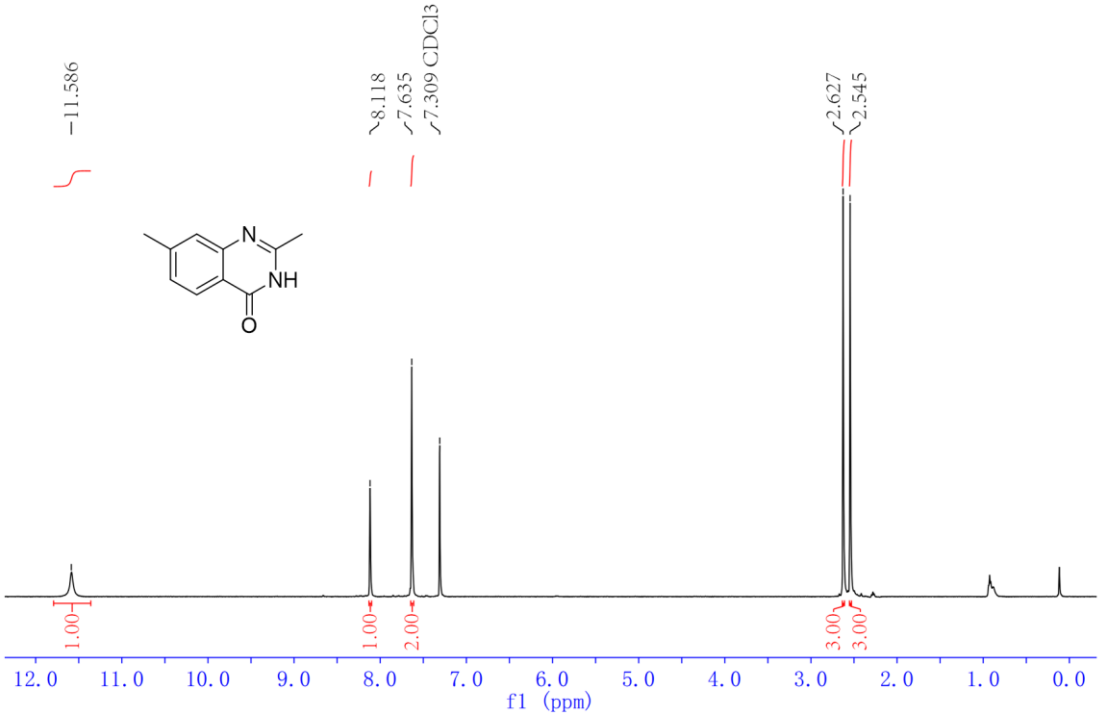

The ^{1}H NMR spectra of **8f**

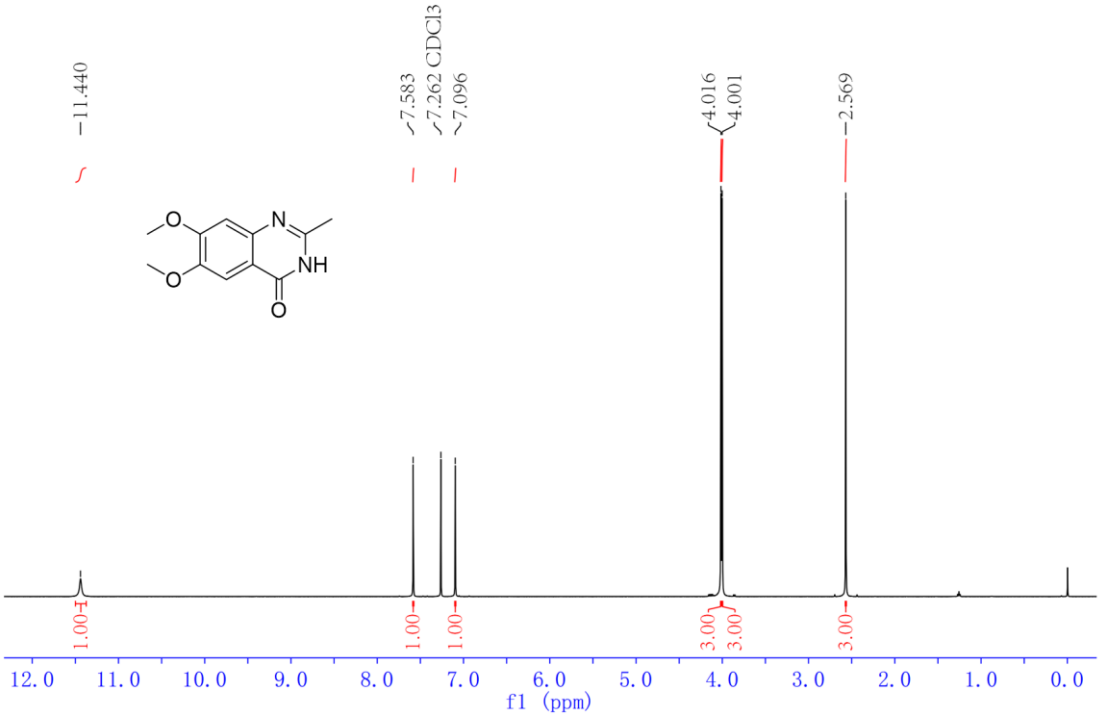

The ^{1}H NMR spectra of **8g**

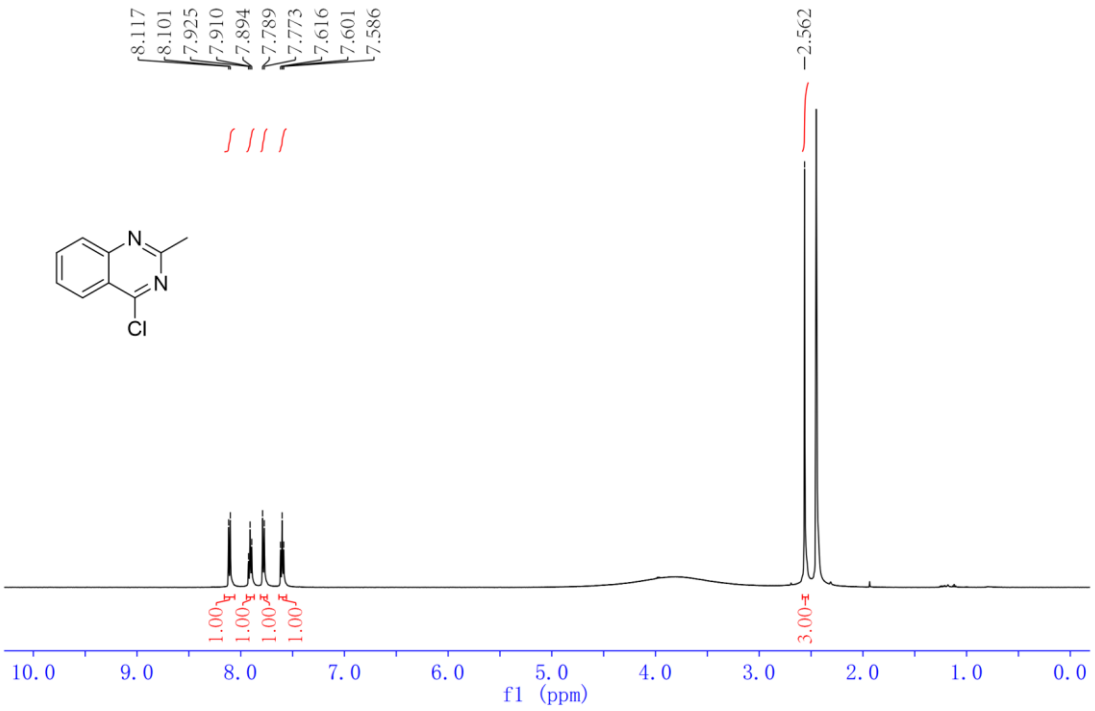

The ^{1}H NMR spectra of **8aa**

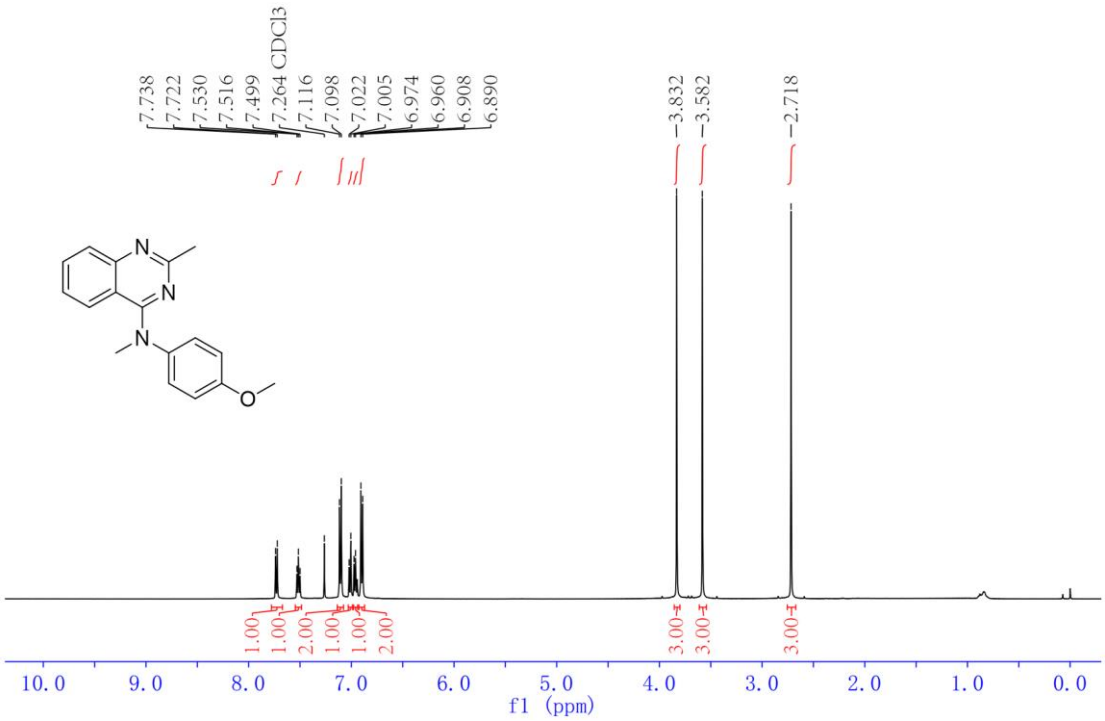

The ^{1}H NMR spectra of **8ab**

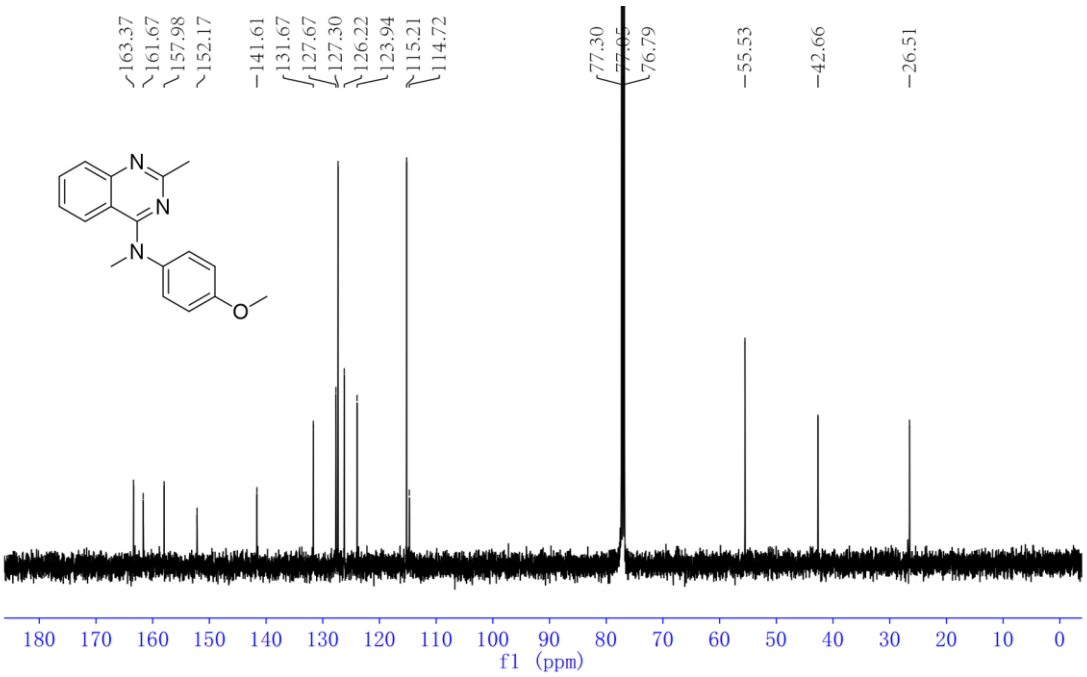

The ^{13}C NMR spectra of **8ab**